INVESTIGATION OF TURBULENT FLOW IN A TWO-DIMENSIONAL CHANNEL

Thesis by

John Laufer

In Partial Fulfillment of the Requirements

For the Degree of

Doctor of Philosophy

California Institute of Technology
Pasadena, California
1948

ACKNOWLEDGEMENTS

I wish to express my most sincere gratitude to Professor Hans Wolfgang Liepmann for his constant encouragement and advice during my graduate studies and research. I further wish to thank Professor Clark B. Millikan for his continuous interest in this research. Discussions on many occasions with Mr. Frank E. Marble were extremely helpful and are hereby greatfully acknowledged. Katja Liepmann and Mehinder Uberoi offered valuable assistance in some of the hot-wire measurements.

Messrs. Leo Davis and Marvin Jessey were responsible for the design and construction of most of the electronic equipment used. This very essential help is much appreciated.

The original draft of the thesis was most deligently prepared by Suzan Laufer. I should also like to thank Mrs Beverley Cottingham, Miss Dorothy Kerns and Miss Alberta Pampeyan for the typing of the final copy of this work and drawing the figures.

Acknowledgement is due to the National Advisory Committee for Aeronautics under whose financial support this work was carried out.

SUMMARY

A detailed exploration of the field of mean and fluctuating quantities in a two-dimensional turbulent channel flow is presented. The measurements were repeated at three Reynolds numbers, 1.23×10^5, 3.08×10^5 and 6.16×10^5, based on the half width of the channel and the maximum velocity. A channel of 5" width and 12:1 aspect ratio was used for the investigation.

Mean speed and axial fluctuation measurements were made well within the laminar sublayer. The semi-theoretical predictions concerning the extent of the laminar sublayer were confirmed. It was found that the viscosity has a more profound influence on the fluctuations than on the mean velocity, the region of influence being approximately four times as wide.

Fluctuations perpendicular to the flow direction v', w' and the correlation coefficient $k = \frac{\overline{u'v'}}{\sqrt{\overline{u'^2}}\sqrt{\overline{v'^2}}}$ were measured, and the turbulent shear distribution calculated. Shear calculations from independent methods using the measured velocity gradient at the wall and pressure gradient along the channel furnished a good check on the values of the shearing stress in all cases with the exception of the highest Reynolds number where τ obtained from the fluctuation measurements is approximately 25% lower. All mean fluctuating quantities were found to decrease with increasing Reynolds number. Measurements of the scales L_y, L_z and micro-scales of turbulence λ_y, λ_z across the channel are presented and their variation

with Reynolds number is discussed. Using a new technique, values for λ_x were obtained; a method for estimating L_x is also given.

The energy balance in the turbulent flow field was calculated from the measured quantities. From this calculation it is possible to give a descriptive picture of turbulent energy diffusion in the center portion of the channel cross-section.

TABLE OF CONTENTS

INTRODUCTION

In recent years a considerable step forward was made in the theory of turbulence. Kolmogoroff (Ref. 1), Heisenberg (Ref. 2) and Onsager (Ref. 3) obtained independently an energy spectrum law that holds in rather restricted types of turbulent flows. This progress gave a new impetus to both theoretical and experimental investigations. The experimental worker may follow two principal methods of approach to the problem. First, he may establish flow fields which satisfy sufficiently the assumptions of the new theory, namely: that the flow is isotropic and of high Reynolds number so that the influence of viscosity is a minimum and the effect of the turbulence producing mechanism is small. Under these conditions he may measure quantities such as correlation functions, scales, and micro-scales that are defined exactly in the flow field and may compare his results to those predicted by the theory. The main difficulty with this method is to predict how closely one has to approximate the actual flow conditions to those assumed in the theory. With other words, the sensitivity of the theory to true isotropic conditions is not known and in case the measurements do not agree with the theory one does not know whether to attribute the disagreement to faulty assumptions in the theory or to the incomplete isotropic conditions of the flow. Furthermore, some recent measurements behind grids at this Institute show that even

with a large increase in Reynolds number the effect of viscosity and grid size have still a pronounced effect over a large frequency range of the spectrum. This indicates that the range of application of the new theory might be outside of the scope of turbulence phenomena encountered in aerodynamics and is of importance in the study of atmospheric turbulence or in the astrophysical field.

The second method of approach is to establish a simple turbulent flow field with well defined boundary conditions and, in the light of the new theories, to try to obtain information on the mechanism of energy transfer from the low frequencies of the energy spectrum to the high ones. The present investigation of a turbulent channel flow has this purpose in mind in its long range program. The difficulties of this method are immediately realized. Because of the non-isotropic nature of the flow, characteristic quantities such as scale and microscale are no longer well defined and it is very possible that in the first stages of the investigation certain quantities will be measured that later prove to be trivial. On the other hand the main advantage of a fully developed channel flow is the fact that, in contrast to the flow behind grids, flow conditions are steady; no decay of mean or fluctuating quantities exists in the direction of the flow. Consequently the turbulent energy goes through all of its stages of transformation across the channel section - turbulent energy production from the mean flow, diffusion,

turbulent and laminar dissipation - and one may study these transformations in detail.

It has become clear that the phenomenological theories of turbulence, such as the mixing length theories, have lost most of their importance. These theories, developed in the late twenties and early thirties, were aimed specifically at an evaluation of the mean velocity distribution in turbulent flow. The existing experimental evidence shows clearly that the mean velocity distribution is very insensitive to the essential assumptions introduced into the phenomenological theories. In fact, purely dimensional arguments generally suffice to give the shape of the mean velocity profile with sufficient accuracy. For the further development of an understanding of turbulence, detailed measurements of the field of fluctuating rather than of mean velocities are necessary. The program of experimental research of which this work is one part is based on this reasoning. It is quite apparent and natural that the same conclusions were drawn by workers in the turbulent field elsewhere, and that in general the main emphasis of present experimental investigation is the exploration of the field of the fluctuating velocity components.

The present set of experiments deals with flow in a two-dimensional channel, i.e. with pressure flow between two flat walls. Channel flow of this type is the simplest type of turbulent flow near solid boundaries which can experimentally be produced.

The simpler Couette type flow requires that one wall move with constant velocity, a condition which is difficult to realize experimentally. It can be approximated by the flow between concentric cylinders but complications due to centrifugal forces arise here. The simple geometry of a two-dimensional channel allows an integration of the Reynolds equations, and the turbulent shearing stress can then be related directly to the shearing stress on the surfaces which, in turn, can be determined from the mean pressure gradient or the slope of mean velocity profile at the wall.

The relation between the apparent stresses and the wall shearing stress can be used to advantage in two fashions. It is here possible to obtain the magnitude of the correlation coefficient responsible for the apparent shear by measuring only the intensities of the turbulent fluctuations. The turbulent shearing stress can also be measured directly by means of hot wire anemometer. A comparison with the shear distribution obtained from mean pressure gradient or velocity profile measurements serves, then, as a very useful check on the underlying assumptions on the one hand, and specifically on the reliability and accuracy of the direct measurements on the other.

Measurements of channel flow have previously been made by Doench (Ref. 4), Nikuradse (Ref. 5), Wattendorf and Kuethe (Ref. 6 and 7) and Reichardt (Ref. 8 and 9). A few measurements have been made recently at the Brooklyn Polytechnical Institute (Ref. 10).

Doench's and Nikuradse's measurements were concerned only with the mean velocity distribution at high Reynolds numbers and are thus of not too much interest for a comparison with the present set of measurements. Wattendorf measured the intensity of the fluctuating velocity components and then deduced the correlation coefficient from the mean pressure measurements. The technique for measuring the axial component of the velocity fluctuation was well developed at the time but the cross component was only tentatively measured.

The most complete set of measurements is due to Reichardt, who measured velocity fluctuations in the direction of the flow and normal to the wall as well as the turbulent shear directly. Reichardt found very good agreement between the shearing stress determined in these two ways; his paper comes closest to the present investigation and his results will be used for comparison. The Reynolds number in Reichardt's measurements was 8,000, lower than the range covered by the present measurements. A criticism which can be made of Reichardt's investigation is his use of a tunnel of only 1:4 aspect ratio. The two-dimensional character of the flow is thus somewhat doubtful. Wattendorf's experiments were made in a channel of very large aspect ratio 18:1 and are thus free of this criticism.

In a preliminary investigation a channel 1" wide and 60" high was chosen. The measurements, however, have shown that in this case the scale of turbulence is so small that great care must be taken to correct the hot wire readings for the effect of

wire length. Measurements of the micro-scales were, in fact, impossible in the 1" channel. The micro-scales were about 0.1 cm and thus of the same order of magnitude as the length of the wire. The corrections for the case of v' and w' measurements were about 30%. Since the method of correction becomes very inaccurate for such large ratios of wire length to micro-scales, the measurements were repeated in a 5" channel with a 12:1 aspect ratio. This ratio was still large enough to insure two-dimensional flow and the length corrections were now of the order of only 3%.

SYMBOLS

x	longitudinal coordinate in the direction of the flow. ($x=0$ corresponds to the channel exit)
y	lateral coordinate. ($y=0$ corresponds to the channel wall)
z	lateral coordinate.
d	half width of the channel (2.5").
δ	thickness of laminar sublayer.
u	mean velocity at any point in the channel.
U_0	maximum value of the mean velocity.
u'	velocity fluctuations in the direction of the mean flow, i.e., x.
v', w'	velocity fluctuations normal to the mean flow in the direction y and z.
$\frac{u'}{U}$	$\equiv \sqrt{\frac{\overline{u'^2}}{U^2}}$, $\frac{v'}{U} \equiv \sqrt{\frac{\overline{v'^2}}{U^2}}$, $\frac{w'}{U} \equiv \sqrt{\frac{\overline{w'^2}}{U^2}}$
p	pressure at any point in the channel.
ρ	air density.
τ	total shearing stress.
τ_0	shearing stress at the wall.
U_τ	$\equiv \sqrt{\frac{\tau_0}{\rho}}$
μ	absolute viscosity of air.
R	Reynolds number based on half width of channel and maximum mean velocity.
$k=\frac{\overline{u'v'}}{\sqrt{\overline{u'^2}\,\overline{v'^2}}}$	correlation coefficient responsible for the apparent shear.
R_x, R_y, R_z	correlation coefficients as functions of X, Y, Z.
$\lambda_x, \lambda_y, \lambda_z$	micro-scales of turbulence.

L_x, L_y, L_z scales of turbulence.

X, Y, Z distances (in the x, y, z direction respectively) between points at which correlation fluctuations are measured.

σ ratio of the square of compensated and uncompensated fluctuations.

M time constant expressing the thermal lag of a hot-wire.

ANALYTICAL CONSIDERATIONS

a) The Equations of Motion for Two-Dimensional Channel Flow: - We denote by u_i and u_i' the mean and fluctuating velocity components respectively, x_i are Cartesian coordinates, p_{ik} denotes the components of the stress tensor which includes both, the viscous and apparent (Reynolds) stresses. The Reynolds equations and the continuity equation for steady flow can thus be written.

$$\rho u_k \frac{\partial u_i}{\partial x_k} = \frac{\partial p_{ik}}{\partial x_k} \tag{1a}$$

$$\frac{\partial u_i}{\partial x_j} = 0 \tag{1b}$$

where

$$p_{ik} = \begin{vmatrix} -p + 2\mu \frac{\partial u_1}{\partial x_1} - \rho \overline{u_1'^2} & \mu\left(\frac{\partial u_1}{\partial x_2} + \frac{\partial u_2}{\partial x_1}\right) - \rho \overline{u_1' u_2'} & \mu\left(\frac{\partial u_1}{\partial x_3} + \frac{\partial u_3}{\partial x_1}\right) - \rho \overline{u_1' u_3'} \\ \mu\left(\frac{\partial u_1}{\partial x_2} + \frac{\partial u_2}{\partial x_1}\right) - \rho \overline{u_1' u_2'} & -p + 2\mu \frac{\partial u_2}{\partial x_2} - \rho \overline{u_2'^2} & \mu\left(\frac{\partial u_2}{\partial x_3} + \frac{\partial u_3}{\partial x_2}\right) - \rho \overline{u_2' u_3'} \\ \mu\left(\frac{\partial u_1}{\partial x_3} + \frac{\partial u_3}{\partial x_1}\right) - \rho \overline{u_1' u_3'} & \mu\left(\frac{\partial u_2}{\partial x_3} + \frac{\partial u_3}{\partial x_2}\right) - \rho \overline{u_2' u_3'} & -p + 2\mu \frac{\partial u_3}{\partial x_3} - \rho \overline{u_3'^2} \end{vmatrix}$$

For channel flow between two parallel flat walls we have

$u_1 = u(y)$
$u_2 = 0$
$u_3 = 0$

$$p_{ik} = \begin{vmatrix} -p - \rho \overline{u'^2} & \mu \frac{du}{dy} - \rho \overline{u'v'} & 0 \\ \mu \frac{du}{dy} - \rho \overline{u'v'} & -p - \rho \overline{v'^2} & 0 \\ 0 & 0 & -p - \rho \overline{w'^2} \end{vmatrix}$$

Where x, y, z and u', v', w' replace the x_i, u_i' etc. for

convenience in writing the now much simpler equations. Equation (1b) is thus automatically satisfied and (1a) becomes:

$$0 = \frac{\partial}{\partial x}\left(-p - \rho\overline{u'^2}\right) + \frac{\partial}{\partial y}\left(\mu\frac{du}{dy} - \rho\overline{u'v'}\right)$$
$$0 = \frac{\partial}{\partial y}\left(-p - \rho\overline{v'^2}\right) + \frac{\partial}{\partial x}\left(\mu\frac{du}{dy} - \rho\overline{u'v'}\right) \qquad (2)$$

In fully developed turbulent flow the variation of mean values of the fluctuating quantities with x should be zero, i.e. the flow pattern is independent of the streamwise direction. Hence, (2) becomes:

$$\frac{1}{\rho}\frac{\partial p}{\partial x} = \nu\frac{d^2u}{dy^2} - \frac{d\overline{u'v'}}{dy} \quad \text{or} \quad \frac{1}{\rho}\frac{\partial p}{\partial x} = \frac{1}{\rho}\frac{d\tau}{dy} \qquad (3a)$$

$$\frac{1}{\rho}\frac{\partial p}{\partial y} = -\frac{\partial\overline{v'^2}}{\partial y} \qquad (3b)$$

Differentiating (3b) with respect to x gives $\frac{1}{\rho}\frac{\partial^2 p}{\partial x\partial y} = 0$ and consequently $\frac{\partial p}{\partial x}$ is independent of y and (3a) is immediately integrable. Thus

$$\frac{y}{\rho}\frac{\partial p}{\partial x} = \nu\frac{du}{dy} - \overline{u'v'} + \text{constant}$$

In the center of the channel the shear vanishes, hence if the channel has the width $2d$ we have

$$\text{constant} = \frac{d}{\rho}\frac{\partial p}{\partial x}$$

and hence:

$$\frac{1}{\rho}\frac{\partial p}{\partial x}(y-d) = \nu\frac{du}{dy} - \overline{u'v'}$$

Or in non-dimensional form:

$$\frac{y-d}{\rho U_o^2}\frac{\partial p}{\partial x} = \frac{\nu}{U_o^2}\frac{du}{dy} - \frac{\overline{u'v'}}{U_o^2} \tag{4}$$

In terms of the shearing stress at the wall,

$$-\frac{\tau_o}{\rho U_o^2}\frac{y-d}{d} = \frac{\nu}{U_o^2}\frac{du}{dy} - \frac{\overline{u'v'}}{U_o^2} \tag{5}$$

It is evident from (4) and (5) that τ_o can be determined in three different ways:

(i) $\tau_o = -d\frac{\partial p}{\partial x}$ — from the mean pressure gradient

(ii) $\tau_o = \mu\left(\frac{du}{dy}\right)_{y=0}$ — from the slope of the mean velocity profile near the wall

(iii) $\tau_o = \frac{(\rho\overline{u'v'} - \mu\frac{du}{dy})d}{y-d}$ — from a direct measurement of $\overline{u'v'}$

if $\frac{y}{d}$ is not too small

$$\mu\frac{du}{dy} \ll \rho\overline{u'v'}$$

and

(iii) $$\tau_o = \rho\overline{u'v'}\frac{d}{y-d}$$

The technically simplest way to determine τ_o, and thus in fact the complete shear distribution, is a measurement of $\frac{\partial p}{\partial x}$. This is the method applied in most investigations.

To determine the slope of the velocity profile near the wall, the profile has to be known up to points very close to the wall, i.e. at least to distances $\frac{y}{d} = 10^{-2}$. This in general requires the use of the hot wire anemometer and very precise measurements.

The third method requires a direct measurement of the correlation between the axial and lateral velocity fluctuations. The technique of this type of measurement is known and was first applied by Reichardt and Skramstad and, in somewhat different form, in recent investigations at the Bureau of Standards, Brooklyn Polytechnical Institute and California Institute of Technology.

In the present investigation all three methods have been applied and the results compared with the exception of the lowest Reynolds number flow. In this case the pressure gradient is extremely small (approximately 0.0003 mm of alcohol per cm) and reasonably accurate measurements were not possible. This comparison of the three methods has the advantage that is gives a good indication of the absolute accuracy of measurements of the fluctuating quantities and the correlation coefficient k.

b) The Phenomological Approach: - The so-called phenomological theories attempt to express the turbulent shearing stress in terms of the mean velocities by introducing some simple physical model to describe the turbulent flow mechanism.

It is seen from equation 3a that if $\tau = \tau(u)$ is known the equation may be integrated and the velocity distribution across the channel in terms of the pressure gradient or wall shear may be obtained.

With the introduction of the "mixing length", l Prandtl put forward the hypothesis (Ref. 11) that

$$\tau = \rho l^2 \left(\frac{du}{dy}\right)\left|\frac{du}{dy}\right| \qquad (6)$$

He assumed that l varies proportionally with the distance from the wall, thus

$$l = cy \qquad \text{where } c \text{ is a constant}$$

Substituting the expression of τ in the integrated form of equation 3a we obtain

$$\tau_0\left(1-\frac{y}{d}\right) = c^2\rho y^2\left(\frac{du}{dy}\right)^2$$

The solution of this differential equation is with the condition that $u = U_0$ at $y = 0$ (Ref. 12)

$$\frac{U_0-u}{U_\tau} = \frac{1}{c}\left[\frac{1}{2}\log\left(\frac{2d}{y}-1\right) - 2\sqrt{\frac{d-y}{d}}\right]$$

While the variation of l with y was obtained by Prandtl from dimensional arguments, Kármán's well known similarity law gives a method for calculating the "mixing length" (Ref. 13). Kármán assumes that l depends only on the local mean velocity gradients and obtains that

$$l = \frac{du}{dy} \Big/ \frac{d^2u}{dy^2}$$

Using this relation together with equations 4 and 6 the mean velocity distribution may be obtained (Ref. 12)

$$\frac{U_0 - u}{U_\tau} = -\frac{1}{A}\left[\log\left(1-\sqrt{1-\tfrac{y}{d}}\right) + \sqrt{1-\tfrac{y}{d}}\right] + B$$ where A and B are constants

the boundary conditions being $\frac{du}{dy} = \infty$ at $y = 0$.

Taylor's vorticity theory can also be applied to find the velocity distribution in a two-dimensional channel, if the variation of the mixing length l with y is assumed. Letting $l = c_1 y$, Taylor obtains (Ref. 14)

$$\frac{U_0 - u}{U_\tau} = \frac{\sqrt{2}}{c_1}\left[\sin^{-1}\sqrt{1-\tfrac{y}{d}} - \sqrt{\tfrac{y}{d}\left(1-\tfrac{y}{d}\right)}\right]$$ where C_1 is a constant

The above equations, although derived from different physical assumptions furnish velocity distributions that agree reasonably well with measured profiles provided the arbitrary constants contained in the equations are rightly chosen. A general discussion of the applicability of these velocity laws may be found in

references 15 and 25. A more detailed analysis of the mixing length theories applied to channel flow is given in reference 12.

c) The Energy Equation:- Writing equation (1a) in the form

$$\rho u_k \frac{\partial u_i}{\partial x_k} = -\frac{\partial p}{\partial x_i} + \mu \nabla^2 u_i$$

we multiply it by u_i

$$\frac{1}{2}\rho \frac{\partial u_i u_i u_k}{\partial x_k} = -\frac{\partial p u_i}{\partial x_i} + \mu u_i \frac{\partial^2 u_i}{\partial x_j \partial x_j}$$

Transforming the last term by partial integration the energy equation of the mean flow becomes

$$\frac{1}{2}\rho \frac{\partial u_i u_i u_k}{\partial x_k} = -\frac{\partial p u_i}{\partial x_i} + \frac{1}{2}\mu \frac{\partial^2 u_i u_i}{\partial x_j \partial x_j} - \mu \left(\frac{\partial u_i}{\partial x_j}\right)\left(\frac{\partial u_i}{\partial x_j}\right) \qquad (7)$$

We may introduce now the velocity perturbations,

$$u_1 = u + u'$$
$$u_2 = v'$$
$$u_3 = w'$$

Since the velocities are independent of the coordinates x and z we obtain after averaging

$$\rho \overline{u'v'}\frac{dy}{dy} + \rho u \frac{d\overline{u'v'}}{dy} + \frac{1}{2}\rho \frac{d}{dy}\overline{v'(u'^2+v'^2+w'^2)} = -u\frac{\partial p}{\partial x} - \frac{\partial \overline{v'p}}{\partial y} + \mu u \frac{d^2 u}{dy^2} + \frac{1}{2}\mu \frac{d^2}{dy^2}\overline{(u'^2+v'^2+w'^2)} - \mu \overline{\left(\frac{\partial u_i'}{\partial x_j}\right)\left(\frac{\partial u_i'}{\partial x_j}\right)}$$

Making use of equation (3a) this simplifies to

$$\tau \frac{du}{dy} = \frac{d}{dy}\left[\rho \overline{v'\left(\frac{u'^2+v'^2+w'^2}{2}\right)} + \overline{v'p}\right] + \mu\left(\frac{du}{dy}\right)^2 - \frac{1}{2}\mu \frac{d^2}{dy^2}\overline{(u'^2+v'^2+w'^2)} + \mu \overline{\left(\frac{\partial u_i'}{\partial x_j}\right)\left(\frac{\partial u_i'}{\partial x_j}\right)}$$

This form was obtained by Kármán (Ref. 16.) while discussing a non-isotropic flow in terms of the statistical theory of turbulence. In order to see the relative orders of magnitudes of the different terms in the equation, Kármán expresses them in terms of a single velocity, $q = \sqrt{u'^2+v'^2+w'^2}$ and a characteristic length D corresponding to the width of the channel. Since

$$\frac{\tau}{\rho} \cong -\overline{u'v'} = O(q^2) \qquad \text{and} \qquad \frac{du}{dy} = O\frac{\sqrt{\tau/\rho}}{D} = O\left(\frac{q}{D}\right)$$

the above equation may be written as

$$A_1 \frac{q^3}{D} = A_2 \frac{q^3}{D} + A_3 \frac{\nu q^2}{D^2} + A_4 \frac{\nu q^2}{D^2} + A_5 \frac{\nu q^2}{\lambda^2}$$

The A_i's have a character of correlation functions. For high Reynolds number flow $\frac{qD}{\nu} \gg 1$, it follows that $\frac{\nu q^2}{D^2} \ll \frac{q^3}{D}$. Thus the second and third term of the right side of the equation may be neglected. Since the pertinent quantities have been measured during the present work the order of magnitude of these terms can be directly evaluated and the omission of the terms is found to be justified. The above equation contains thus only terms of the form $\frac{q^3}{D}$ and $\frac{\nu q^2}{\lambda^2}$; they should be of the same order of magnitudes, therefore $\frac{q\lambda^2}{\nu D} = O(1)$. It is of considerable interest to see whether experimental results confirm this relation. Taking as an example results from the measurements at $R = 30,800$ and $\frac{y}{d} = 0.5$

$$q = 52 \text{ cm/sec}, \quad \lambda_y = 0.5 \text{ cm} \quad \therefore \quad \frac{q\lambda^2}{\nu D} = \frac{52 \times 0.25}{0.155 \times 12.7} = 10.5$$

This ratio seems to be fairly constant for different Reynolds numbers and across the channel cross-section.

In wiew of the above dimensional considerations, the energy equation may be written

$$\tau \frac{du}{dy} = \frac{d}{dy}\left[\overline{v'\left(\frac{u'^2+v'^2+w'^2}{2}\right)} + \overline{v'p}\right] + \mu \overline{\left(\frac{\partial u_i'}{\partial x_j}\right)\left(\frac{\partial u_i'}{\partial x_j}\right)} \qquad (8)$$

The equation expresses the fact that the energy produced by the turbulent shear forces at a certain point is partly diffused and partly dissipated. This equation has been used in estimating the energy diffusion across the channel, since from the measured quantities the production term and dissipation can be calculated.

EQUIPMENT AND PROCEDURE

1. Wind Tunnel: - The investigation was carried out in the wind tunnel shown in figure 1. The turbulence level is controlled by a honeycomb and seamless precision screens, followed by an approximately 29:1 contraction. The screens have 18 meshes per inch and a wire diameter of 0.018". The honeycomb consists of paper mailing tubes, 6" long and 1" in diameter.

The overall length of the channel is 23'. At the entrance section it is 3" wide having an aspect ratio of 20:1. In a distance of 7' it expands to a width of 5" reducing the aspect ratio 12:1. The walls of the exit portion of the channel (about 6') are made of 3/4" thick plywood with a 1/4" birch inside cover. They were specially treated in order to acquire smooth finish, and were reinforced to avoid warping (figure 2); in spite of this a few percent of width variation existed.

The tunnel is operated by a 62 horsepower stationary, natural gas engine - normally operating at a fraction of its rating - which drives two 8-blade fans. The speed is remotely controlled by means of a small electric motor which drives the throttle through a gear and lead screw system.

The experiments were carried out at speeds of 3, 7.5 and 15 meters per second.

2. Traversing Mechanism: - Figure 3 shows the type of mechanism used during the experiments. It consists simply of a micrometer screw on which the hot wire support is fastened. The support can rotate freely in a plane perpendicular to the air flow thus enabling one to adjust the hot wire exactly parallel to the wall.

The zero reading of the traversing mechanism $(y=0)$ was carefully found using the following method: the hot wire was placed close to the wall (approximately 0.025 cm away); the distance between the wire and its image in the polished wall was measured by means of an ocular micrometer. The position of the wire is, of course, one-half of the observed distance, and could be determined with an accuracy of ± 0.0005 cm.

In order to obtain the pressure distribution along the middle of the channel a 6' long thin walled tube 3/8" in diameter was used with a small static pressure hole drilled close to its end. The tube was free to slide in a support at the entrance of the channel so that the position of the pressure hole relative to the channel exit could be changed. The tube was kept straight and under tension by means of weights.

3. Hot-Wire Equipment: - All velocity measurements were made with hot-wire anemometers. The frequency response of the amplifier-compensator unit of the hot-wire equipment (figures 25 and 26) is flat from approximately 2 to 10,000 cycles, using a 0.00024" wire at standard operating conditions.

The compensation of the hot-wire for thermal lag is accomplished by a capacity network. The range of time constants was chosen from 0.3 to 1 milliseconds corresponding to the characteristics of a 0.00024" wire at the operating conditions employed in general at GALCIT. No attempt was made to extend the range of compensation to larger values of M since in this case the noise level soon becomes appreciable.

The correct setting of the compensating unit was found using the square wave method described recently by Kovásznay (Ref. 17). The time constants of the wires used for turbulence measurements fell between 0.4 and 0.9 milliseconds.

The output readings were taken with a thermocouple and precision potentiometer.

a) Mean Speed Measurements:

A half mil (0.0005") platinum wire of 1 cm length was used. The measurements were made by the constant resistance method. This method has the advantage of keeping the wire temperature constant through the velocity field.

b) Turbulence Measurements:

For the investigation of turbulent fluctuations, 0.00024"

Wollaston wire was used. The wire was soft soldered to the tips of fine sewing needles after the silver coating had been etched off. The two lateral components v' and w' and the correlation coefficient $k = \frac{\overline{v'w'}}{\sqrt{\overline{v'^2}\,\overline{w'^2}}}$ were measured using the X wire technique. The method was essentially the same as described in detail in previous reports from this laboratory. It is realized that the use of an X meter does not permit measurements very close to the wall.

The X meters for shear maasurements had angles between the wires of approximately 90°. The angles of the v', w' meter were of the order of 30°. The wire length of the u' meter was about 1.5 mm that of the v' meter was 3 mm.

The parallel wire technique used recently at the Brooklyn Polytechnic Institute was also tried in order to obtain the lateral component of the velocity fluctuation and the shear close to the wall. The double wire instrument is superior to the X meter since it allows an exploration of the turbulent field up to distances of a few thousands of an inch from the wall. However, it was found impossible to obtain reliable values with this instrument. The corrections due to u' fluctuations and due to unequal heating of the wires were pronounced and not easily accountable. The method was therefore temporarily abandoned after considerable time and labor was spent on it.

c) Measurements of Correlations Between Two Points:

The correlation functions between values of u' points along the

y and z axis, i.e.

$$R_y = \frac{\overline{u'(0)\,u'(Y)}}{\sqrt{\overline{u'(0)^2}}\sqrt{\overline{u'(Y)^2}}}$$

$$R_z = \frac{\overline{u'(0)\,u'(Z)}}{\overline{u'^2}}$$

were measured using the standard technique. The scales of turbulence L_y , L_z and the micro-scales λ_y , λ_z at different points across the channel were obtained from these measurements.

d) Measurements of λ_x :

A new technique for the measurement of λ_x has been applied. The method is based on a paper by Rice* (Ref. 18). Rice expresses the average number of zero values of a random fluctuation, $I(t)$ per unit time in terms of the correlation function

$$\psi(t') = \overline{I(t)\,I(t+t')} \qquad \text{where } t' \text{ is a time interval}$$

He obtains that:

the average number of zeros of $I(t)$ per unit interval =

$$= \frac{1}{\pi}\sqrt{\frac{-\psi''(0)}{\psi(0)}} \tag{9}$$

the restriction on $I(t)$ being: $I(t)$ and $\frac{\partial I(t)}{\partial t}$ are distributed normally (Gaussian distribution).

Dr. A. Erdelyi** gave a rigerous mathematical proof, different

---

*Dr. H. L. Dryden drew the attention of the GALCIT group to this paper.

**During a seminar given at the California Institute of Technology in May, 1948.

from Rice's, of this relation using a method described by Kac (Ref. 19) and gave a generalization of Rice's result, namely:

the average number of c values of $I(t)$ per unit interval =

$$= \frac{e^{-\frac{c^2}{\psi(0)}}}{\pi} \sqrt{\frac{-\psi''(0)}{\psi(0)}}$$

Translating Rice's result into our notation $\left(I \equiv u',\ t \equiv \frac{x}{U_o}\right)$ we obtain, since $R_x(0) = 1$

$$\sqrt{-\frac{\partial^2 R_x}{\partial x^2}} = \frac{1}{\lambda_x} = \frac{\pi \times \text{the ave. no. of zeros of } u' \text{ per second}}{U_o}$$

Thus by counting the zeros of an oscillograph trace of the u' fluctuations, λ_x may be calculated directly assuming a normal distribution for both u' and $\frac{\partial u'}{\partial x}$. It is known that the distribution of u' is closely a Gaussian one even in non-isotropic turbulence (see for instance Ref. 20), however, for the case of $\frac{\partial u'}{\partial x}$ Townsend reports a small deviation from the normal distribution (Ref. 21). For the preliminary measurements of λ_x reported presently, no corrections were applied as yet for this effect. Figure 4 shows an oscillograph trace of the u' fluctuation in the middle of the channel at R = 30,800. The trace represents an interval of approximately 1/100 second. It should be noted that a different method of measuring λ_x is described recently by Townsend (Ref. 21).

e) Measurement of L_x :

The following simple procedure was applied to obtain a rough

estimate of scale of turbulence corresponding to correlations between points along the x axis: denote by $F(n)$ the fraction of turbulent intensity which is contributed by frequencies between n and $n+dn$, i.e.

$$\overline{u'(n)^2}\,dn = F(n)\,dn$$

and thus

$$\int_0^\infty F(n)\,dn = 1$$

Consider now an uncompensated hot-wire. If the time constant of the wire is M, the response will be

$$\left[\overline{u'(n)^2}\right]_{uncomp.}$$

where

$$\left[\overline{u'(n)^2}\right]_{uncomp.} = \frac{\overline{u'(n)^2}}{1+M^2n^2}$$

The total intensity will then be given by

$$\left[\overline{u'^2}\right]_{uncomp.} = \overline{u'^2}\int_0^\infty \frac{F(n)\,dn}{1+M^2n^2} \quad *$$

Thus, if the ratio of the reading of the same wire compensated and uncompensated is denoted by σ, we have

$$\frac{1}{\sigma} = \int_0^\infty \frac{F(n)}{1+M^2n^2}\,dn \qquad (10)$$

*Formula of this general type have been proposed by Kampe de Feriet and Frenkiel for determining the spectrum of turbulence from non-compensated hot-wire measurements by varying M.

In order to estimate L_x , $F(n)$ is assumed to have the simple form

$$F(n) = \frac{2}{\pi} \frac{\frac{L_x}{U_o}}{1 + n^2 \frac{L_x^2}{U_o^2}}$$

which was given by Dryden (Ref. 22) and corresponds to an exponential correlation curve.

Then

$$\frac{1}{\sigma} = \frac{2}{\pi} \int_0^\infty \frac{\frac{L_x}{U_o}}{\left(1 + n^2 \frac{L_x^2}{U_o^2}\right)\left(1 + M^2 n^2\right)} dn$$

or with

$$\eta = \frac{L_x n}{U_o} \quad , \quad \alpha = \frac{M U_o}{L_x}$$

$$\frac{1}{\sigma} = \frac{2}{\pi} \int_0^\infty \frac{d\eta}{(1+\eta^2)(1+\alpha^2\eta^2)} = \frac{1}{1+\alpha}$$

Hence

$$L_x = \frac{M U_o}{\sigma - 1}$$

Thus by measuring the ratio of the mean squares of the fluctuating velocities with and without compensation L_x can be estimated.

The procedure was checked in the flow behind a 1/2" grid where the lateral scale was measured and where due to isotropy

the relation $L_x = 2L_y$ should hold fairly well.

The results were:

$$\sigma = 1.85$$
$$M = 7 \times 10^{-4} \text{ sec} \qquad \therefore L_x = 1.24 \text{ cm}$$
$$V_o = 1.5 \times 10^{3} \text{ cm/sec}$$

Direct measurements gave $L_y = 0.553$ cm. Hence $L_x = 1.11$ cm which shows that this method of estimating the value of L_x is satisfactory.

PRELIMINARY MEASUREMENTS IN A ONE INCH CHANNEL

In the initial stages of the turbulent channel flow investigation a channel of 1" cross-section was used. Measurements of mean and fluctuating velocities and of the correlation coefficient k were completed. The scales L_y and L_z were also measured at the channel center and were found to be about 0.2 to 0.3 cm. This small scale turbulence existing in the channel imposed a definite limitation on the accuracy of the fluctuating measurements. Wire length corrections as high as 30% had to be applied to the v' and w' measurements. Furthermore, no micro-scales could be measured accurately; thus one of the objectives of the investigation, the calculation of the energy dissipation across the channel could not be obtained. Nevertheless, results show good consistency: the three independent measurements of the turbulent shear indicate satisfactory agreement.

It is of interest to present these preliminary measurements, the Reynolds number of which was 12,200, and to compare them with those obtained in the 5" channel. Figure 5 shows the distribution of all the measured quantities in the 1" channel and it may be directly compared to figure 17 showing the quantities measured in the 5" channel at the same Reynolds number.

Although the slopes of the mean velocities at the wall are almost the same in each case $\left[\frac{\tau_o}{\rho U_o^2}\ (\text{of } 1") = 0.0019;\ \frac{\tau_o}{\rho U_o^2}\ (\text{of } 5") = 0.0018\right]$, the velocity ratios $\frac{u}{U_o}$ in the 5" channel seem to be lower across

most part of the channel. This indicates that a more intense turbulent energy production takes place in the 5" channel (energy production is $\tau \frac{du}{dy}$). Indeed, comparing the turbulent velocity fluctuations $\frac{u'}{U_o}$, $\frac{v'}{U_o}$, and $\frac{w'}{U_o}$, they increase at a faster rate - especially $\frac{u'}{U_o}$ - toward the wall in the wider channel, although their values at the channel center check very well in the two cases. The shear distribution $\frac{\tau}{\rho U_o^2}$ is almost the same for the two channels; it follows therefore, from the relation

$$\frac{\overline{u'v'}}{U_o^2} = k \frac{u'}{U_o} \frac{v'}{U_o}$$

that k must have a higher value in the 1" channel since there both $\frac{u'}{U_o}$ and $\frac{v'}{U_o}$ are smaller. Indeed the maximum value of k in this case is 0.6, while in the 5" channel is 0.5.

As a matter of interest it could be mentioned that if the basis of comparison is not Reynolds number but maximum mean speed $[U_o \text{ (of 1")} = 15 \text{ m/sec}]$ then figure 5 shows a very similar distribution of u', v', and w' to that of figure 19, the absolute values being somewhat lower in the 5" channel.

RESULTS AND DISCUSSION

1. Mean Velocity Distribution: - A careful study of the two-dimensional nature of the channel flow was first made. Mean velocity measurements were carried out at approximately $x = -2$ inches at different heights in the channel: at positions 6" from the bottom, 6" from the top and at the middle. Agreement among the three sets of measurements confirmed the two-dimensionality. A further check was made on possible end effects that might influence the results. The channel was extended by 6" and the mean velocity measurements were repeated at $x = -8$ inches. No change in the profile was noticed. Figure 6 shows the mean velocity distributions at three Reynolds numbers; R = 61,600, 30,800 and 12,300. The distributions follow Kármán's logarithmic law very well, except, of course, near the wall and at the center of the channel (figure 7). The values of U_τ were obtained from the velocity gradients at the wall.

Measurements were made with special care close to the wall. Velocities at a large number of points were recorded within the laminar sublayer in order to establish with reasonable accuracy the shape of the velocity profile at the wall (figure 8). The thickness of the laminar sublayer was found to be: $\delta \simeq 30\nu/U_\tau$ (figure 7) as found by other investigators (Ref. 5).

In figure 8 it can be seen that for the case of the lowest Reynolds number a few points near the wall indicate very low

velocities. Since the $\frac{y}{a}=0$ point has been determined with great accuracy and since the equations of motion of the channel flow require a negative curvature for the velocity profile, one had to conclude that the hot-wire indicates too low velocities near the wall. (The dotted curve shows the interpolated velocity distribution for $0<\frac{y}{a}<.01$.) It can be shown that very high local velocity fluctuations cause the hot-wire to read velocities lower than the true mean value. Since the mean voltage of the wire varies with the square-root of the velocity we may write

$$\sqrt{U} = \sqrt{\bar{U}}\,\overline{\left(1+\frac{u'}{\bar{U}}\right)^{1/2}}$$

where U is the velocity to which the hot-wire responds, $\bar{U}$ is the true mean velocity. Expanding the expression

$$\sqrt{U} = \sqrt{\bar{U}}\left(1-\frac{1}{8}\frac{u'^2}{\bar{U}^2}-\cdots\right)$$

Since the average of the odd terms is zero the series converges rapidly. In the region in question, the velocity fluctuations are very high indeed $\left(\frac{u'}{\bar{u}}>0.30\right)$, nevertheless the method of correction indicated above is not sufficient to establish the required negative curvature for the profile. The reason for the appearance of the inflection points is at present not completely understood. Further efforts will be made in the near future to clear up this point.

2. Turbulence Levels: - Figures 10-15 represent the results of measurements of the three components u', v', w' of the turbulent velocity fluctuation distribution in the channel for the three Reynolds numbers.

The u' velocity fluctuations relative to local speeds increases extreemly rapidly near the wall as shown in figures 10 and 11. Measurements very close to the wall indicate that $\frac{u'}{u}$ reaches a maximum well within the laminar boundary layer $\left(\frac{y_{max}\, v_t}{\nu} \cong 4\right)$ and it tends toward a constant value at the wall which is independent of the Reynolds number.

The absolute values of the u' distribution shows the same general shape as obtained by Reichardt (Ref. 9), having the characteristic maximum near the wall showing the strong action of viscosity even for values of $y \cong 4\delta$.

Using the X type hot-wire technique for obtaining the velocity fluctuation components v' and w', no measurements could be obtained near the wall. Figures 14 and 15 show that while in the center of the channel the magnitudes of v' and w' are the same, w' increases faster toward the wall. This agrees with the ultramicroscope measurements in a pipe of Fage and Townsend (Ref. 23).

No length corrections were applied to the u' measurements since the scale L_x was much larger than the wire length, except possibly near the wall where scale measurements could not be made. In this region, however, the fluctuations are very large and the absolute values given in figure 11 must be accepted with

reserve. The hot-wire response for large velocity fluctuations is not well understood yet and no correction was attempted. A small length correction (3%) using values computed by Zebb* was applied to the v' and w' measurements.

*Zebb, K. California Institute of Technology Thesis 1942. Unpublished.

3. Correlation Coefficient and Shear Distribution: - The correlation coefficient is fairly constant across most part of the channel (figure 16) as indicated already by Wattendorf and Kuethe (Ref. 6). The maximum values of k obtained decrease slowly with increasing Reynolds number, thus showing a definite Reynolds number dependence. Existing results indicate, however, that parameters other than Reynolds numbers also influence the value of k. The following table shows magnitudes of the maximum correlation coefficient as obtained by different investigators working with channels of various widths and with various Reynolds numbers;

Experiments by	Channel Width (cm)	R	$-k_{max}$
Reichardt	24.6	8,000	0.45
Laufer	2.5	12,200	0.63
Laufer	12.7	12,300	0.50
Wattendorf	5.0	15,500	0.52
Laufer	12.7	30,800	0.45
Laufer	12.7	61,600	0.40

Wattendorf obtained his value of k from his measurements of the quantities $\frac{u'}{U_c}$, $\frac{v'}{U_c}$ and $\frac{\overline{u'v'}}{U_c^2}$. Unfortunately his preliminary measurements of v' are incorrect: their magnitude is larger than that of u' at all values of y across the channel contrary to results obtained by Reichardt and the present writer. Wattendorf, himself, points out the inaccuracy of the v' values in his paper. Because of the large values of v' his computed correlation coefficients are too low. The value $k=0.52$ listed in the above table was obtained by using Wattendorf's value $\frac{\overline{u'v'}}{U_c^2}=0.001$ and $\frac{u'}{U_c}=0.055$ and the

value $\frac{v'}{U_o}=0.035$ $(\frac{y}{d}=0.5)$ obtained by the author for both the 1" (2.5 cm) and 5" (12.7 cm) channel at R = 12,3000.

The variation of k indicates that for the same Reynolds number the correlation coefficient tends to increase with increasing maximum mean velocity (i.e. in a channel of decreasing width).

Figures 17-19 show the distribution of all the measured quantities including the shear distribution. For the case of the two higher Reynolds numbers three independent measurements were made for the determination of the shear distribution by methods indicated on page 11 . In the lowest Reynolds number flow no pressure measurements were made because the very low pressure gradient (approximately 0.0003 mm of alcohol per cm) did not permit accurate measurements. Figure 9 indicates that consistent results are obtained for the value of τ whether calculated from the pressure gradient along the channel or form the velocity gradient at the wall. In comparing the turbulent shear distributions obtained from hot-wire measurements and calculated from $\left(\frac{du}{dy}\right)_{y=0}$, figures 17 and 18 show satisfactory agreement. However, for the highest Reynolds number flow the hot-wire measurements gave a 25% lower value for the shear coefficient as seen in figure 19. At the present, the writer can give no satisfactory explanation for this discrepancy.

4. Scale and Micro-Scale Measurements: - For a further understanding of the structure of the turbulent field correlations of u' fluctuations at two different points were carried out. Since the field is not isotropic, the measurements were repeated both in the y and z direction for different values of $\frac{y}{d}$.

a) R_z Correlations:

Figures 20 shows two typical R_z distributions at station $\frac{y}{d} = 1.0$ and $\frac{y}{d} = 0.7$ corresponding to R = 30,800. It is seen that small correlations still exists at distances $Z = 5.0\,cm$; for larger values of Z inaccuracies of the measurements did not permit the exploration of the negative region of the correlation distribution. From the measured distributions of R_z at four stations across the channel, the values of L_z and λ_z were calculated, (figures 22 and 23). L_z is seen to be decreasing uniformly toward the wall, while λ_z reaches a definite maximum at about $\frac{y}{d} = 0.7$ and then it decreases with decreasing $\frac{y}{d}$.

b) R_y Correlations:

Because of the existance of gradients for both mean and fluctuating quantities in the y direction, the magnitude of L_y obtained from the correlation curves cannot be considered as accurate as those of L_z and λ_z . Correlation distributions at a given value of $\frac{y}{d}$ were obtained by fixing the stationary hot-wire at the given value of $\frac{y}{d}$ and traversing with the moving hot-wire away from the fixed one toward the channel center. L_y and λ_y were then calculated from these R_y distributions.

In the region $1.0 > \frac{y}{d} > 0.1$ the gradients of the various quantities are slight and the relative constant value of L indicates that there exists no significant asymmetry in the $R_y(Y)$ function. Measurements of the top part of the R_y distribution $(1 > R_y > 0.8)$ by Prandtl and Reichardt (Ref. 24) justify fairly well this belief.

The distribution of λ_y across the channel (figure 23) is similar to that of λ_z. From $\frac{y}{d} = 1.0$ to $\frac{y}{d} \cong 0.7$ they increase almost proportionally to u' indicating that the turbulent energy dissipation $\left(W \sim \frac{u'^2}{\lambda^2} \right)$ is approximately constant in this region. It should be noticed, however, that λ_z is consistently larger than λ_y throughout the channel cross-section. This shows that the flow is not isotropic even in the channel center. Some measurements of λ_y close to the wall are also indicated in figure 21.

The distribution of L_y (figure 22) shows a more complicated behaviour. The scale decreases toward the wall in the region $1.0 > \frac{y}{d} > 0.7$ reaching a minimum at $\frac{y}{d} \cong 0.7$, and only after obtaining a maximum at approximately $\frac{y}{d} = 0.4$ does it decrease toward $\frac{y}{d} = 0$. Figure 21 shows clearly that traversing from $\frac{y}{d} = 1.0$ toward $\frac{y}{d} = 0.7$, the correlation coefficient R_y after a slowly decreasing curvature at $Y = 0$ (increasing λ_y) drops to zero at a faster rate resulting in a lower value of L_y. The dotted curve measured at $\frac{y}{d} = 0.4$ shows the considerably increased correlations for larger values of Y at this station, which explains the reason for the large L_y scale at this point.

It is seen thus that around $\frac{y}{d} = 0.7$ there is a definite decrease in energy content of the fluctuations having low frequencies. Further consideration of this fact is given later during the discussion of the energy balance in the channel. No length correction was found to be necessary for the obtained values of λ_y and λ_z.

Rough estimate of L_x by the method already described gave a value approximately twice of L_z at the center of the channel (figure 22). Its value increases to a maximum at $\frac{y}{d} \cong 0.5$ and then decreases rapidly. No values for L_x are given for the lowest Reynolds number; in this case, namely, the value of σ is very close to unity and since L_x is proportional to $\frac{1}{\sigma - 1}$, σ should be known within a 1% accuracy to give consistent results for L_x. Unfortunately measurements of σ cannot be made with this accuracy particularly when the u' fluctuations are of rather low frequencies as in the case for R = 12,800. It should be mentioned that the accuracy of the determination of L_x is more limited by the inaccurately measured value of σ rather than by the fact that an approximate spectrum function, $F(n)$, is used in equation 10.

For a matter of interest the results of some preliminary measurements of λ_x are indicated in figure 23. It is seen that its value is close to that of λ_z for the two higher Reynolds numbers and seems to be somewhat high for R = 12,300.

5. Reynolds Number Effect: - Figure 6 shows the distribution of mean velocities plotted in the form of "friction velocity" $\frac{u}{U_\tau}$ versus "friction distance parameter" $\frac{U_\tau y}{\nu}$. In this form the profiles are independent of the Reynolds number $\frac{U_0 d}{\nu}$ and follow Kármán's logarithmic law:

$$\frac{u}{U_\tau} = A \log \frac{y U_\tau}{\nu} + B$$

The constants A and B are 5.5 and 5.2 respectively as compared to 5.75 and 5.0 in the experiments of Doench (Ref. 4) and Nikuradse (Ref. 5). It is also seen that the action of viscosity becomes noticable for $\frac{U_\tau y}{\nu} \leq 30$ as obtained by Nikuradse.

The Reynolds number has a definite influence on the velocity fluctuations also. Along most part of the cross-section where the influence of the viscosity is negligible the fluctuations u', v' and w' decrease slowly with increasing Reynolds number. Since in this region the product $k\frac{v'}{U_0}$ increases approximately the same rate as $\frac{u'}{U_0}$ (with the exception near the channel center) we may write

$$\frac{\tau}{\rho U_0^2} = k \frac{u'}{U_0} \frac{v'}{U_0} = \text{constant} \frac{u'^2}{U_0^2}$$

This relation was already pointed out by Wattendorf and Kuethe (Ref. 3).

The action of viscosity near the wall is very pronounced on the u' fluctuations. Its influence seems to be stronger on the

fluctuating quantities than on the mean velocity. $\frac{u'}{U_o}$ starts to increase very rapidly at about $\frac{U_o y}{\nu} = 100$ already and reaches a characteristic maximum at approximately $\frac{U_o y}{\nu} = 22$.

Figure 11 shows the u' distributions relative to local speeds near the wall. It is seen that after reaching a maximum they tend to a finite value (about 0.018) at the wall, which value seems to be independent of the Reynolds number. This same value was obtained during measurements in a 1" channel. It should be mentioned that already Taylor pointed out, based on Fage and Townsend's ultra-microscope measurements, that $\frac{u'}{U}$ and $\frac{w'}{U}$ approach a finite value at the wall (Ref. 23).

It is of considerable interest to discuss the variation of the scale and micro-scale with Reynolds number. For flows behind grids where the turbulence is isotropic the scale is independent of the mean velocity and depends on the mesh size of the grid. Similar behavior was found to be true for the channel flow too. Figure 22 shows the distributions of L_y and L_z for different velocities. They indicate no consistent variation with velocity. Furthermore measurements in a one inch channel gave a five times lower value for L_z and a somewhat larger ratio for L_y , than the values obtained in the present investigation.

The variation of λ-s depends, of course, on the velocity and channel width. They decrease with increasing velocity; however, their variation with channel width is slower than that of L .

6. Fully Developed Character of the Turbulence: - The flow in the channel is called fully developed if the variations of the mean values of the velocity and the mean squares of the velocity fluctuations with x are vanishingly small. That the mean velocity profile does not vary downstream is evident from the pressure gradient measurements (figure 9). The gradient in x of $\overline{u'^2}$ was measured on the axis of the channel. It was found that $\overline{u'^2}$ was indeed decreasing with x . The gradient, however, was very small as compared with $\frac{1}{\rho}\frac{\partial p}{\partial x}$:

$$\frac{\partial \overline{u'^2}}{\partial x} \cong 0.01 \frac{1}{\rho}\frac{\partial p}{\partial x}$$

Hence for all practical purposes $\frac{\partial \overline{u'^2}}{\partial x}$ can be neglected. No measurements have been made concerning $\frac{\partial \overline{u'v'}}{\partial x}$, since the scatter in the values would cover any effect. However, there is little doubt that $\frac{\partial \overline{u'v'}}{\partial x}$ is of the same order as $\frac{\partial \overline{u'^2}}{\partial x}$ and that the use of equations 3 is therefore justified here.

7. Energy Balance in the Fluctuating Field: - The energy equation in a two-dimensional channel has the form as given by equation 8:

$$\tau \frac{du}{dy} = \frac{d}{dy}\left[\overline{\rho v'\left(\frac{u'^2+v'^2+w'^2}{2}\right) + v'p}\right] + \mu\overline{\left(\frac{\partial u_i'}{\partial x_j}\right)\left(\frac{\partial u_i'}{\partial x_j}\right)}$$

This equation is valid throughout the cross-section of the channel with the exception of a small region near the wall. The term on the left side of the equation corresponds to the energy produced by the shearing stresses and it can be obtained directly from the measurements of τ and the mean velocity profile. The second term on the right expresses the amount of energy that is being dissipated due to the breaking down of the larger eddies to smaller ones. The term may be written explicitly

$$W = \mu\left\{2\overline{\left(\frac{\partial u'}{\partial x}\right)^2} + 2\overline{\left(\frac{\partial v'}{\partial y}\right)^2} + 2\overline{\left(\frac{\partial w'}{\partial z}\right)^2} + \overline{\left(\frac{\partial v'}{\partial z} + \frac{\partial w'}{\partial y}\right)^2} + \overline{\left(\frac{\partial w'}{\partial y} + \frac{\partial v'}{\partial z}\right)^2} + \overline{\left(\frac{\partial u'}{\partial z} + \frac{\partial w'}{\partial x}\right)^2}\right.$$

The problem is to express these functions in terms of easily measurable quantities. In case of isotropic turbulence Taylor solved the problem by introducing the micro-scale of turbulence, λ, and obtains for the dissipation

$$W = 15\,\mu\,\frac{u'^2}{\lambda^2} \qquad (9)$$

It is attempted to carry over his analysis for the case of channel flow. The following assumptions have to be made in this connection:

a) The gradient of the velocity fluctuations is small in all three directions. With the exception of the region near the wall this is justifiable from the measurements.

b) Since only u' correlations have been measured, it is assumed that the v' , w' correlations as functions of Y and Z respectively (Kármán's f functions) have the same curvature at the origin $(Y=Z=0)$ as the u' correlation as function of X ; that is

$$\left(\frac{\partial^2 R_y^{v'}}{\partial Y^2}\right)_0 = \left(\frac{\partial^2 R_z^{w'}}{\partial Z^2}\right)_0 = \left(\frac{\partial^2 R_x^{u'}}{\partial X^2}\right)_0 = -\frac{1}{\lambda_x^2}$$

Furthermore the v' correlations as functions of X , Z , and w' correlations as functions of X (Kármán's g functions) have the same curvature at the origin as the u' correlation as function Z ; i.e.

$$\left(\frac{\partial^2 R_x^{v'}}{\partial X^2}\right)_0 = \left(\frac{\partial^2 R_z^{v'}}{\partial Z^2}\right)_0 = \left(\frac{\partial^2 R_x^{w'}}{\partial X^2}\right)_0 = \left(\frac{\partial^2 R_z^{u'}}{\partial Z^2}\right)_0 = -\frac{2}{\lambda_z^2}$$

Finally, since the y direction is a distinguished direction because of the gradients of the velocities we put

$$\left(\frac{\partial^2 R_y^{w'}}{\partial Y^2}\right)_0 = \left(\frac{\partial^2 R_y^{u'}}{\partial Y^2}\right)_0 = -\frac{2}{\lambda_y^2}$$

It should be noted that these assumptions do not require locally isotropic conditions.

3. The cross products were calculated using similar arguments;

thus

$$\overline{\frac{\partial v'}{\partial x}\frac{\partial u'}{\partial y}} = -\frac{1}{2}\frac{v'}{\lambda_z}\frac{u'}{\lambda_y} \quad , \quad \overline{\frac{\partial w'}{\partial y}\frac{\partial v'}{\partial z}} = -\frac{1}{2}\frac{w'}{\lambda_y}\frac{v'}{\lambda_z} \quad , \quad \overline{\frac{\partial u'}{\partial z}\frac{\partial w'}{\partial x}} = -\frac{1}{2}\frac{u'}{\lambda_z}\frac{w'}{\lambda_z}$$

4. λ_x was obtained at the channel center only; its variation with y was assumed to be proportional to that of λ_z .

With these assumptions the derivatives of the fluctuations could be expressed in terms of the measured values of λ_x , λ_y and λ_z :

$$W = \mu\left[\frac{2}{\lambda_x^2}\left(\overline{u'^2}+\overline{v'^2}+\overline{w'^2}\right) + 2\frac{\overline{v'^2}}{\lambda_z^2} - \frac{\overline{u'v'}}{\lambda_z\lambda_y} + 2\frac{\overline{u'^2}}{\lambda_y^2} + 2\frac{\overline{w'^2}}{\lambda_y^2} - \frac{\overline{v'w'}}{\lambda_y\lambda_z} + 2\frac{\overline{v'^2}}{\lambda_z^2} + 2\frac{\overline{u'^2}}{\lambda_z^2} - \frac{\overline{u'w'}}{\lambda_z^2} + 2\frac{\overline{w'^2}}{\lambda_z^2}\right]$$

At the middle of the channel W turned out to be 2.37 erg/cm^3sec for R = 30,800. Using the isotropic relation

$$W = 15\mu\frac{\overline{u'^2}}{\lambda_y^2} = 15\mu\frac{\overline{u'^2}}{\lambda_x^2}$$

values 3.93 and 1.67 erg/cm^3sec , were obtained depending whether λ_y or λ_x is used. (For the value of u' the algebraic mean of the squares of the fluctuations was used.)

Figure 24 shows the distribution of W across the channel section. Taylor obtained similar distribution of the dissipated energy across the channel (Ref. 26), however, his numerical magnitudes are too high since he used the isotropic relation with the values of λ_y in equation 9 which turns out to be less than both λ_x and λ_z .

From the known distributions of the energy production and

dissipation the diffusion of energy is easily calculated from equation 8. It is seen from figure 24 that at $\frac{y}{a} \cong 0.7$ the diffusion term is zero. It was also pointed out earlier that in this region the R_y correlations show a considerable change in shape indicating a shift in energy from the lower to higher frequencies of the velocity fluctuations. These two facts suggest the possibility that the energy diffusion is associated mainly with the low frequencies of the fluctuations.

The equation expressing the balance of the three forms of energy furnishes us with the following picture of the turbulent flow field in the channel where viscous dissipation is still negligible: two planes passing through points where the diffusion of energy vanishes divide the channel flow into three parts. From these planes energy is being transported toward the channel center and the walls. The middle region, the width of which is of the order of L_x receives most of its energy by diffusive action and this energy is dissipated here at a constant rate. In the two outside regions all three energy terms increase rapidly, the production term being the dominent one, and their interaction is more involved.

This picture of the flow field is only of a descriptive nature. The purpose of further investigations will be to obtain information on how such an energy balance develops and what is its mechanism.

CONCLUDING REMARKS

The measurements presented here confirm the general conceptions concerning the mean velocity profile in a turbulent channel. The extension of the laminar sublayer, the velocity profile in the sublayer, and the trnsition layer to the logarithmic velocity distribution as measured here are in good agreement with general theoretical expectations.

Measurements of the turbulent field show that the hot wire technique is well enough developed to give consistent results for the intensities and double correlation functions.

Detailed measurements of the u' velocity fluctuations were carried out well within the laminar sublayer. It was found that the magnitude of $\frac{u'}{u}$ approaches a constant value at the wall (approximately 0.18) the value being independent of the Reynolds number. The magnitudes of the v' and w' fluctuations are nearly the same in the middle region of the channel, w' increasing more rapidly toward the wall.

The measured microscales λ_x , λ_y and λ_z are of the same order of magnitudes, λ_y being somewhat smaller however their value compared to the scales is rather large. The distribution of λ_y, λ_z shows a consistent maximum at $\frac{y}{d} = 0.7$; they increase proportionally with u' indicating a constant rate of energy dissipation in the center portion of the channel (since $W \sim \frac{u'^2}{\lambda^2}$).

The scales L_y, L_z in the center region are independent of U_c and depend only on the channel width. The microscales however show a dependency on the Reynolds number.

From the calculated magnitudes of the energy produced by the shearing stresses and of the dissipated energy a descriptive picture of the energy diffusion across the channel is obtained.

REFERENCES

1. Kolmogoroff, A. N.: - The Local Structure of Turbulence for Very Large Reynolds Number. C. R. (Doklady), Ac. Sc. U.S.S.R. 30, No. 4, (1941) p. 301.

2. Heisenberg, W.: - Zur Statistischen Theorie der Turbulence. Unpublished- 1946.

3. Onsager, L.: - The Distribution of Energy in Turbulence. Abstract-Physical Review II, 68, (1945) p. 286.

4. Doench, F.: - Divergente und Konvergente Turbulente Stroemungen mit Kleinen Oeffnungswinkeln. Heft 282 der Forschungsarbeiten auf dem Gebiete des Ingenieurwesens (1926).

5. Nikuradze, I.: - Stroemung des Wassers in Konvergenten und Divergenten Kanaelen. Heft 289 der Forschungsarbeiten auf dem Gebiete des Ingenieurwesens (1929).

6. Wattendorf, F. L. and Kuethe, A. M.: - Investigations of Turbulent Flow by Means of the Hot-Wire Anemometer. Physics, Vol. 5 (1934) pp. 157-160.

7. Wattendorf, F. L.: - Investigation of Velocity Fluctuations in a Turbulent Flow. Jour. Aero. Sci. 3 (1936) pp. 200-202.

8. Reichardt, H.: - Die Quadratischen Mittelwerte der Laengsschwankungen in der Turbulenten Kanalstroemung. Z.A.M.M., 13 (1933) pp. 177-180.

9. Reichardt, H.: - Messungen Turbulenter Schwankungen. Naturwissenschaften, Vol. 26, (1938) p. 404.

10. Harrington, Margosian, Heller: - New Hot-Wire Instrumentation for the Investigation of Shearing Stress and Correlations in Turbulent Boundary Layers. Final report for Contract NAW-2665.

11. Prandtl, L.: - Bericht uber Untersuchungen zur Ausgebildeten Turbulenz. Z.A.M.M. Vol. 5, (1925) pp. 137-138.

12. Goldstein, S.: - Modern Developments in Fluid Dynamics. Vol. II, Oxford (1943) pp. 337-358.

13. v. Kármán, Th.: - Mechanische Aehnlichkeit und Turbulenz. Nachr. Ges, Wiss. Goettingen, (1930) p. 68.

14. Taylor, G. I.: - Flow in Pipes and Between Parallel Planes. Proc. Roy. Soc. A, Vol. 159 (1937) p. 501.

15. Millikan, C. B.: - A Critical Discussion of Turbulent Flows in Channels and Circular Pipes. Proc. Fifth International Congress of Appl. Mech. (1938) pp. 386-392.

16. v. Kármán, Th.: - The Fundamentals of Statistical Theory of Turbulence. Jour. Aero. Sci., Vol. 4, (1937) pp. 131-138.

17. Kovásznay, L.: - Calibration and Measurement in Turbulence Research by the Hot-Wire Method. (1943) T.M. No. 1130.

18. Rice, S. O.: - Mathematical Analysis of Random Noise. The Bell System Tech. Journal, Vol. 23, No. 23 (1946) p. 282.

19. Kac, M.: - On the Average Number of Real Roots of a Random Algebraic Equation. Bull Am. Math. Soc. Vol. 49, No. 4 (1943)

20. Townsend, A. A.: - Measurements in the Turbulent Wake of a Cylinder. Proc. Roy. Soc. A, Vol. 190 (1947) p. 555.

21. Townsend, A. A.: - The Measurement of Double and Triple Correlation Derivatives in Isotropic Turbulence. Proc. Cambridge Phil. Soc. Vol. 34 (1948) p. 565.

22. Dryden, H. L.: - Turbulence Investigations at the National Bureau of Standards. Fifth International Congress of Applied Mechanics, (1938).

23. Fage, A. and Townend, H. C. H.: - An Examination of Turbulent Flow with an Ultramicroscope. Proc. Roy. Soc. A, Vol. 135 (1932) 657-677.

24. Prandtl and Reichardt: - Deutsche Forschung, Part 21 (1934) pp. 110-121.

25. v. Mises, R.: - Some Remarks on the Laws of Turbulent Motion in Tubes. von Karman Anniversary Volume, 1941.

26. Taylor, G. I.: - Statistical Theory of Turbulence. Proc. Roy. Soc. A 151 (1935), 455-464.

FLOW DIAGRAM OF THE TWO-DIMENSIONAL TUNNEL

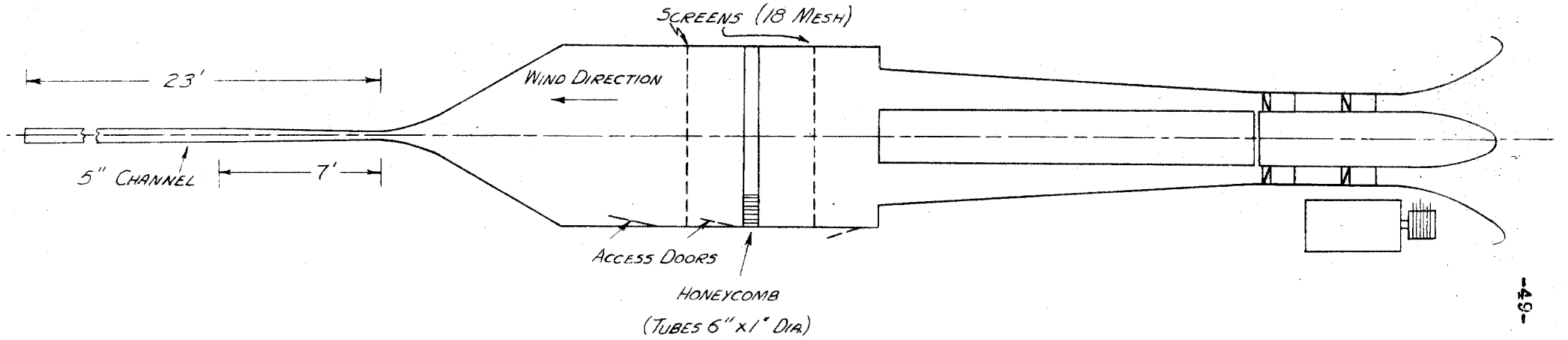

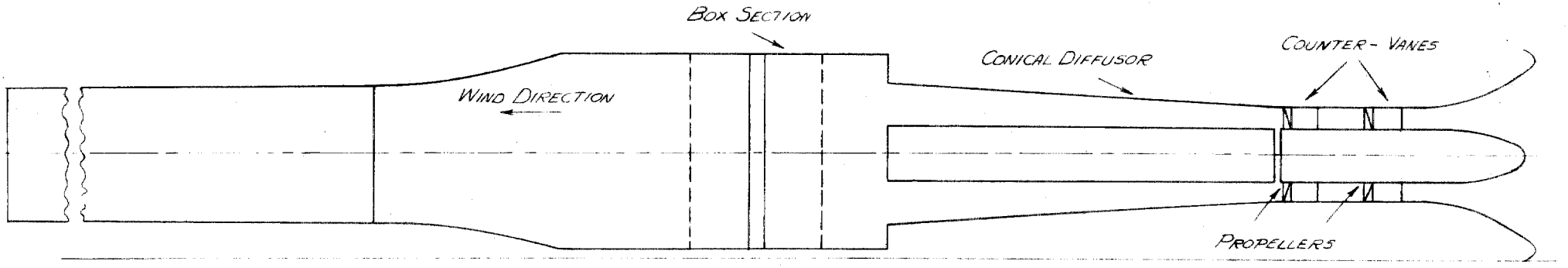

SCALE: $\frac{3''}{16} = 1'$

FIG

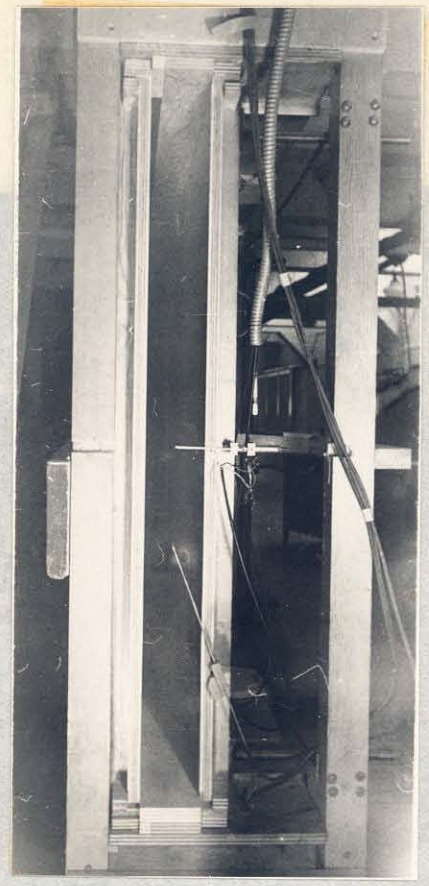

Figure 2

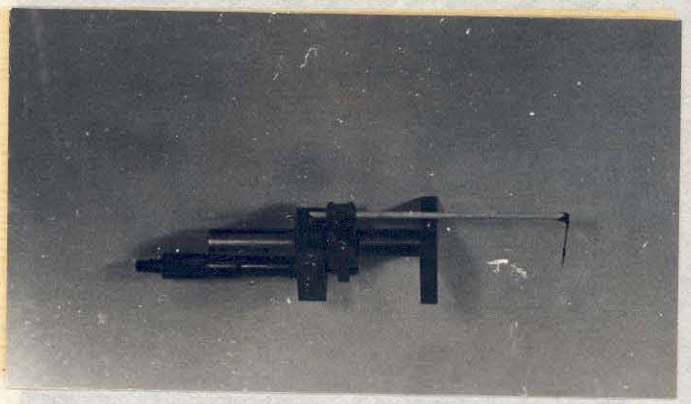

Figure 3

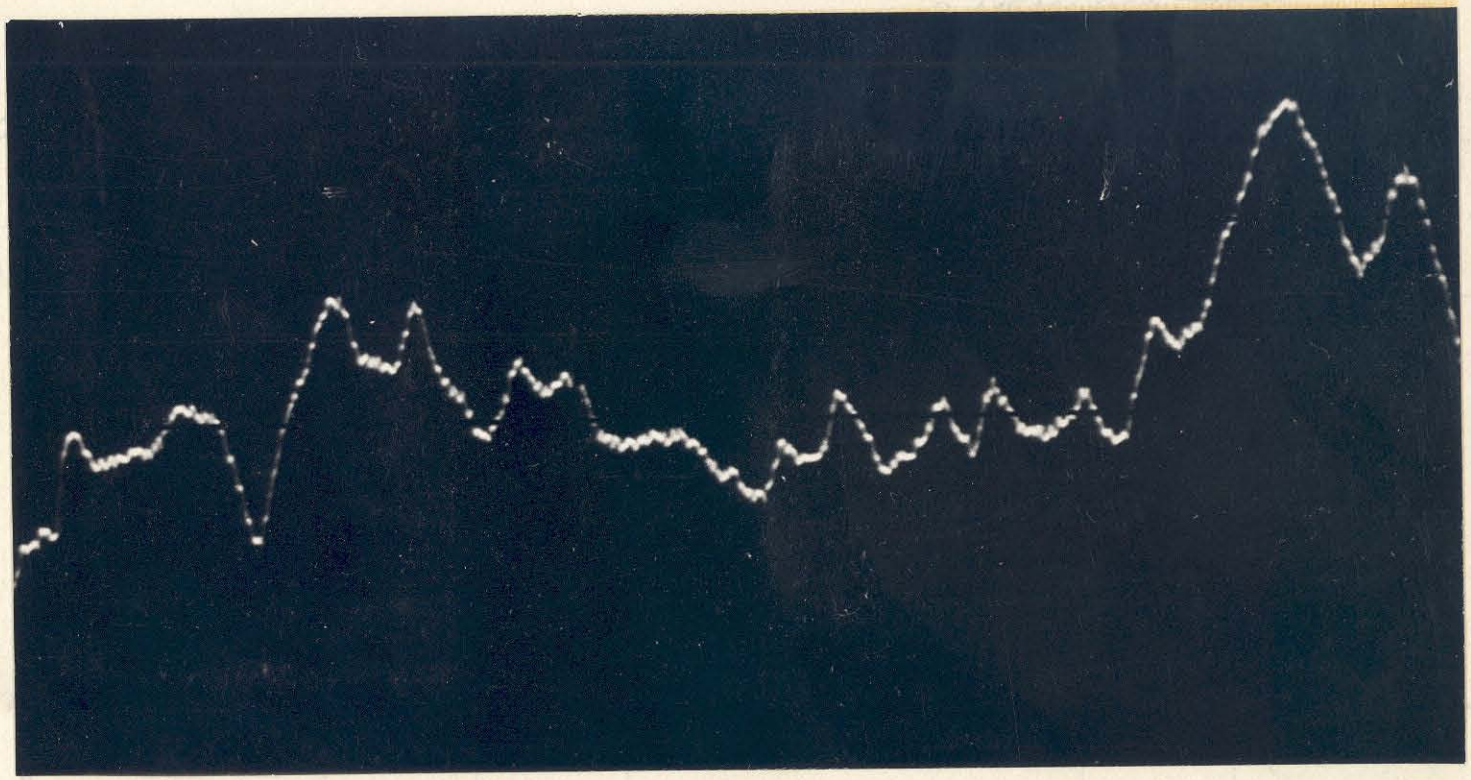

Figure 4

Horizontal Line Corresponds to u'(t) = 0

DISTRIBUTION OF THE MEASURED QUANTITIES ACROSS THE TWO DIMENSIONAL CHANNEL OF ONE INCH CROSS-SECTION

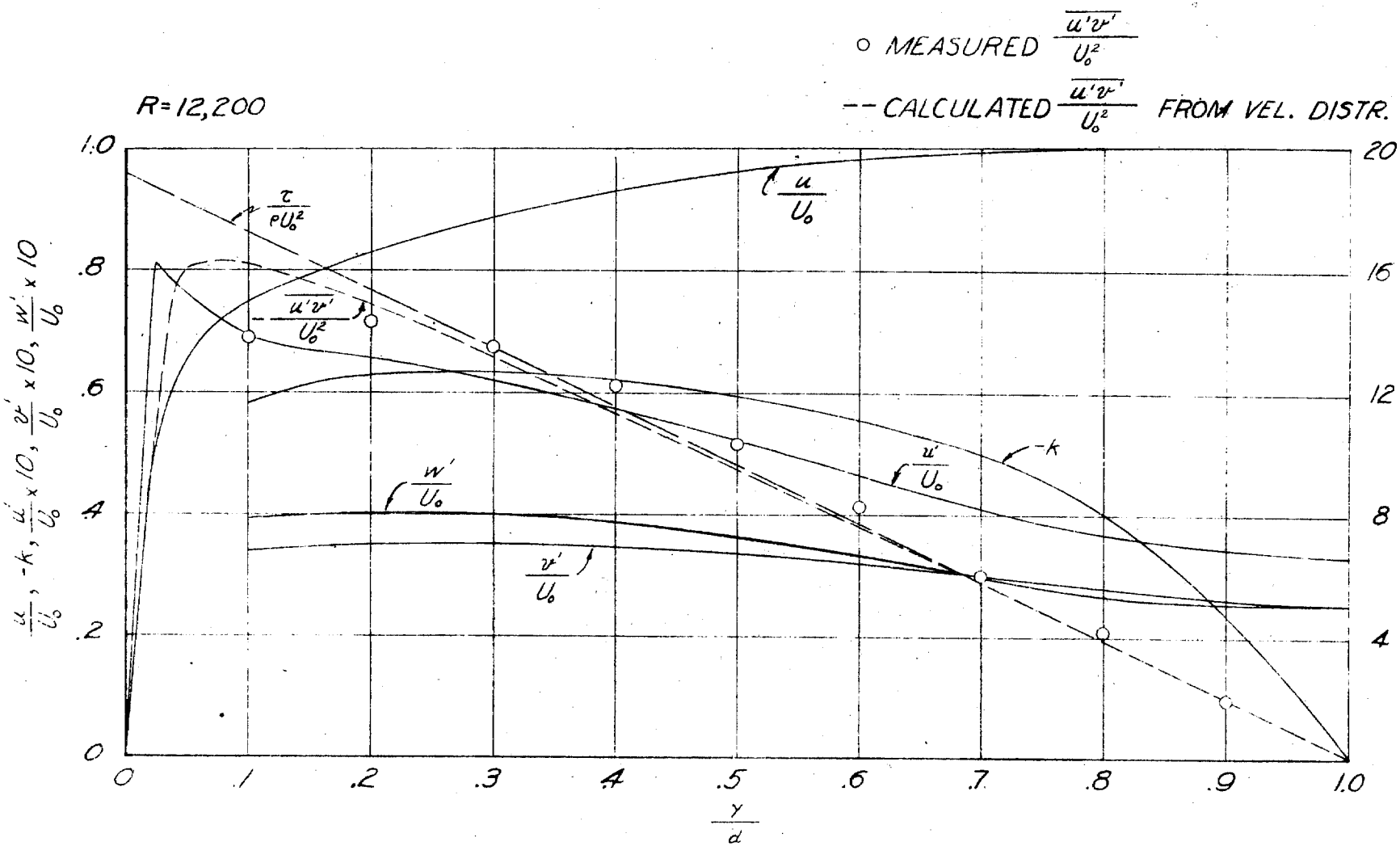

FIG. 5

FIG. 6.

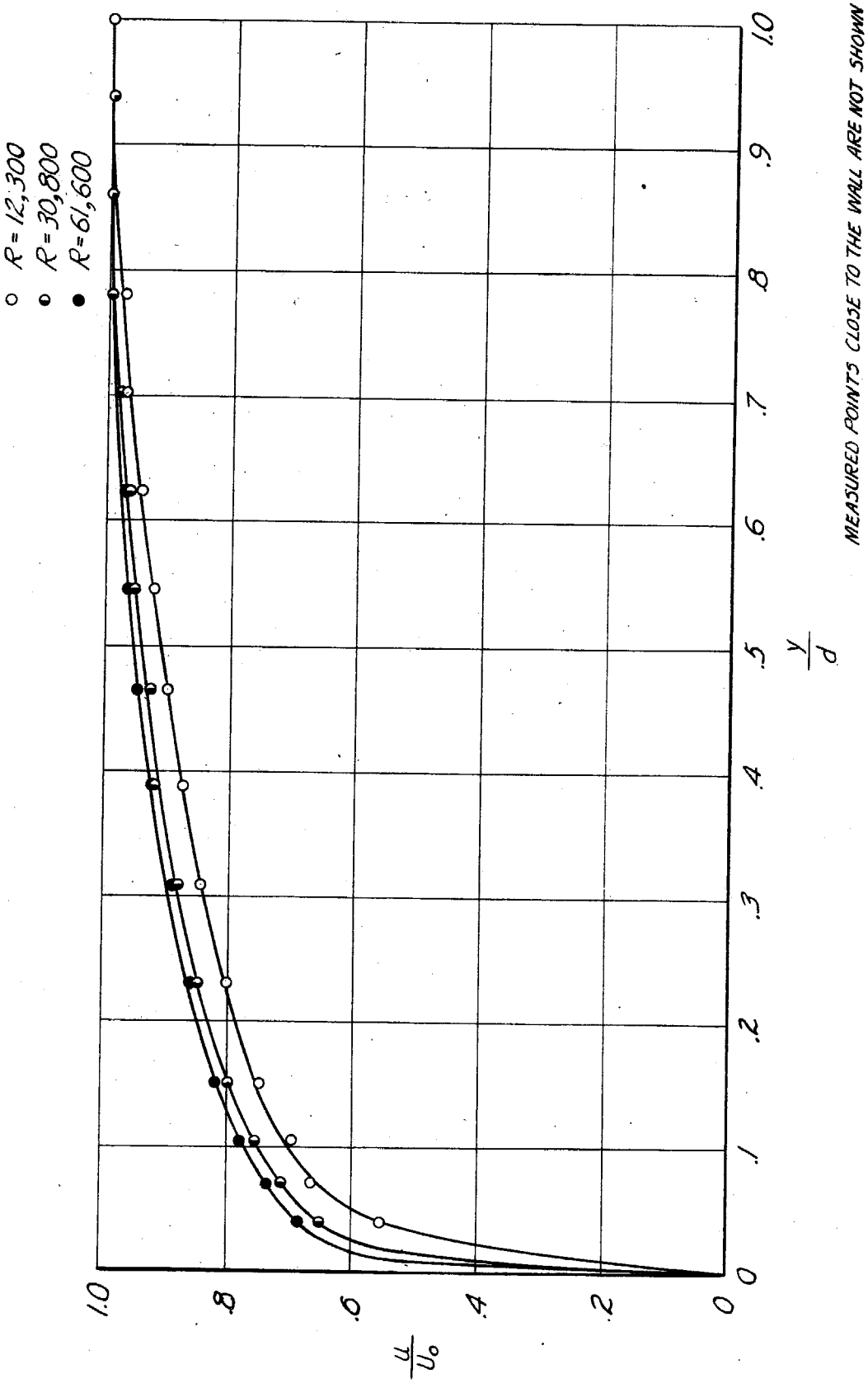
MEAN VELOCITY DISTRIBUTION
R = 12,300
R = 30,800
R = 61,600
u/U₀
y/d
0
.1
.2
.3
.4
.5
.6
.7
.8
.9
1.0
MEASURED POINTS CLOSE TO THE WALL ARE NOT SHOWN

LOGARITHMIC REPRESENTATION OF THE MEAN VELOCITY DISTRIBUTION

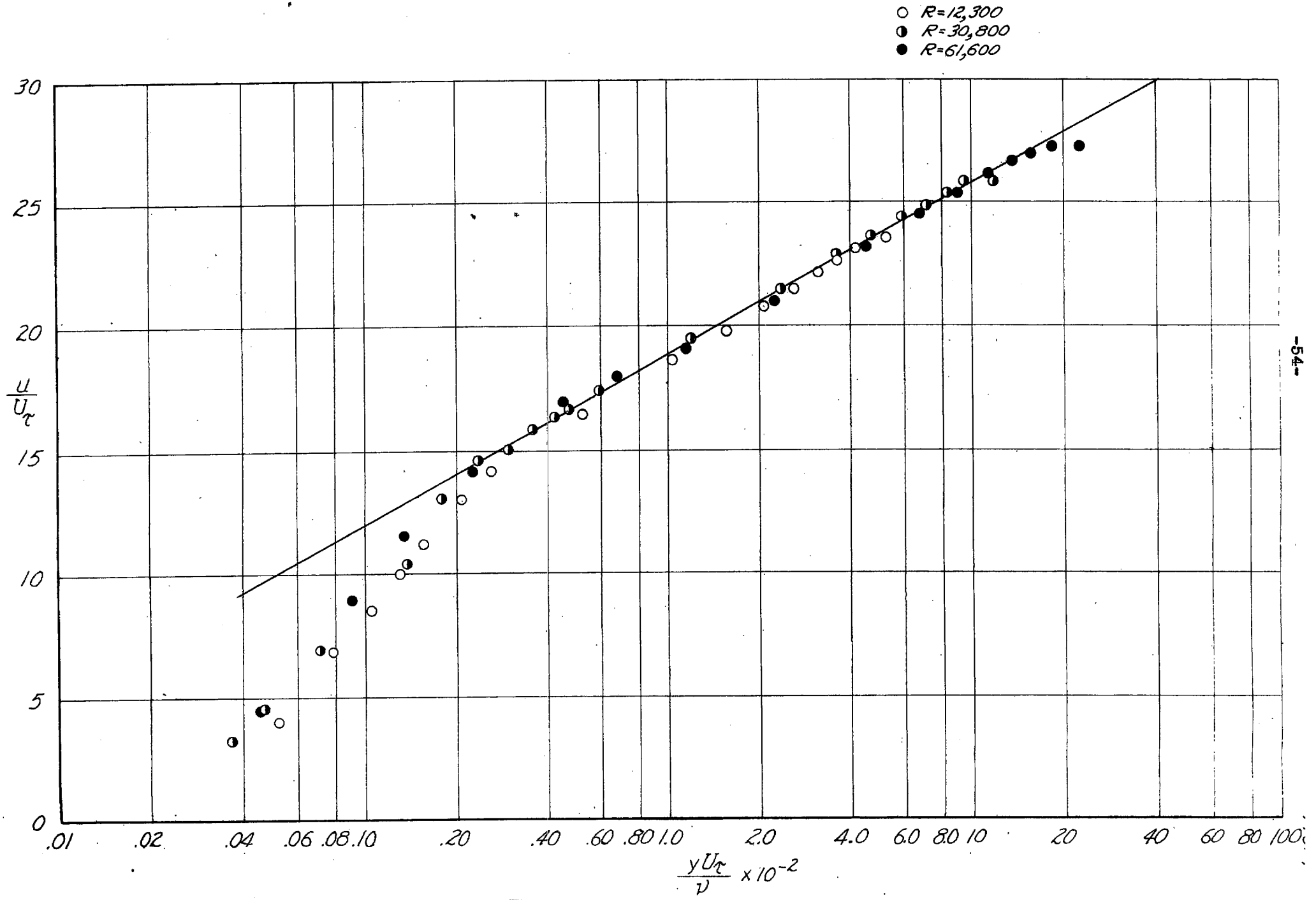

FIG. 8

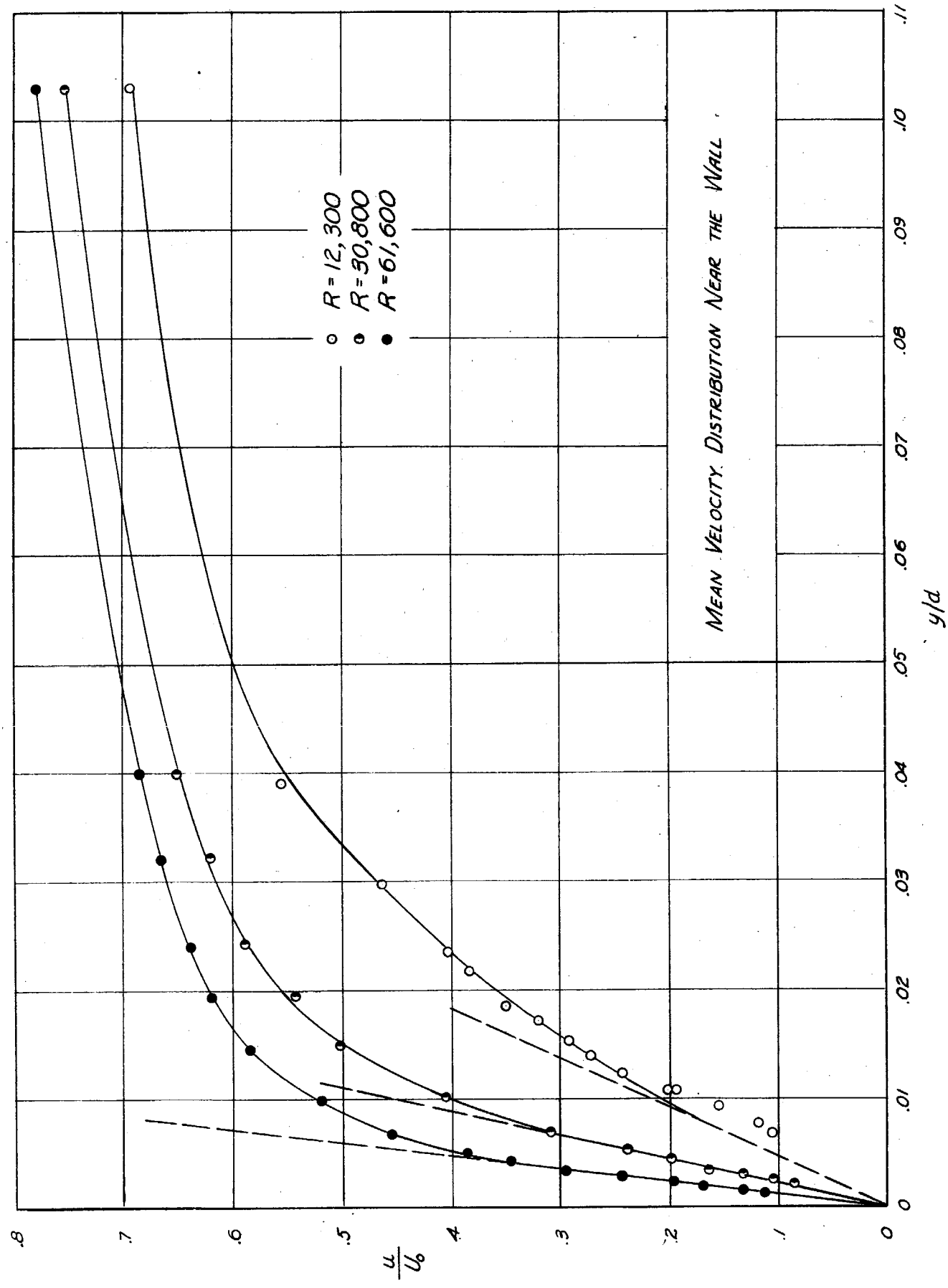
MEAN VELOCITY DISTRIBUTION NEAR THE WALL
R = 12,300
R = 30,800
R = 61,600
u/U
y/d
0
.1
.2
.3
.4
.5
.6
.7
.8
.01
.02
.03
.04
.05
.06
.07
.08
.09
.10
.11

Pressure Distribution Along the Channel

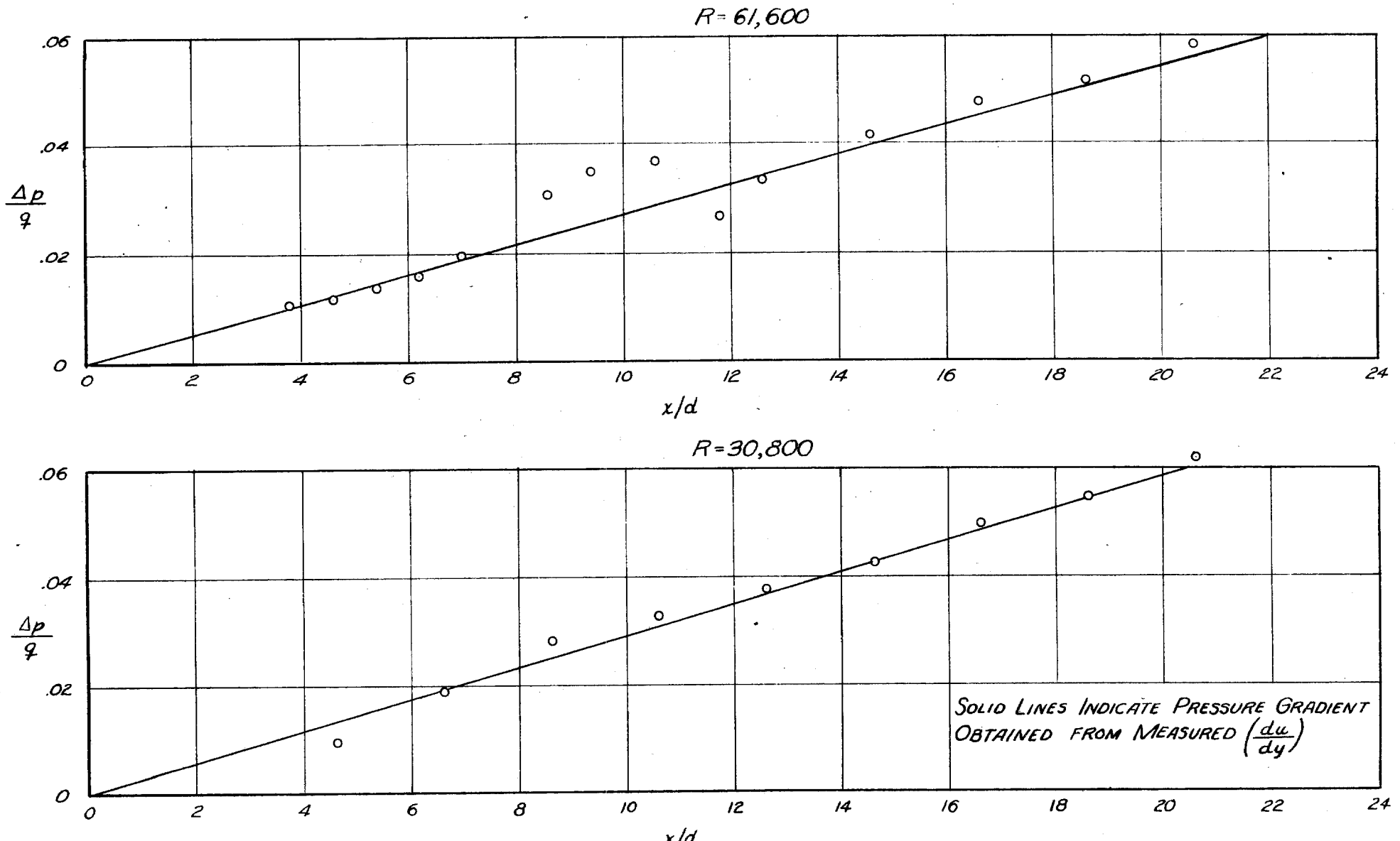

Fig. 9

FIG. 10

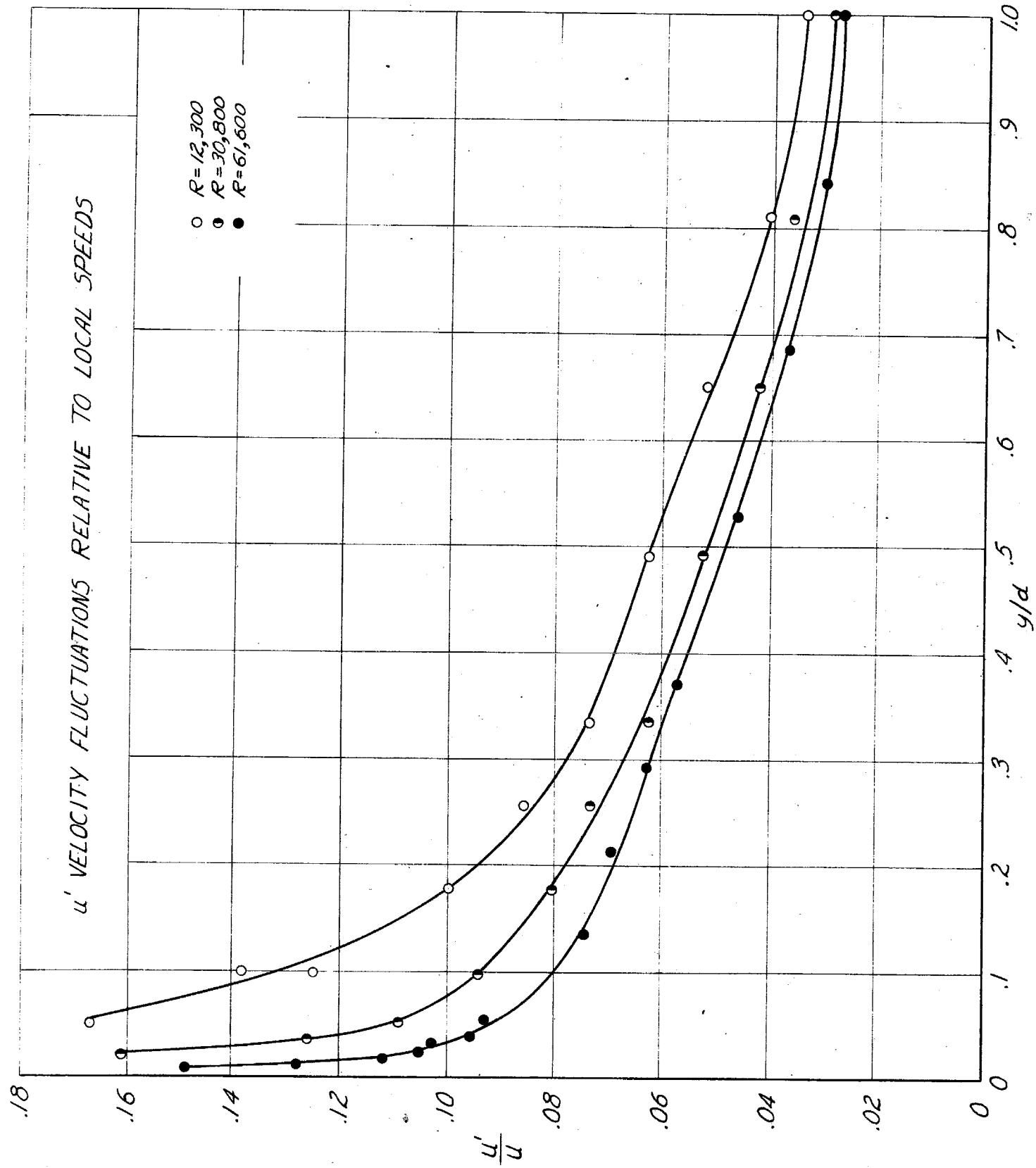
u' VELOCITY FLUCTUATIONS RELATIVE TO LOCAL SPEEDS
R=12,300
R=30,800
R=61,600
u'/u
y/d
.18
.16
.14
.12
.10
.08
.06
.04
.02
0
.1
.2
.3
.4
.5
.6
.7
.8
.9
1.0

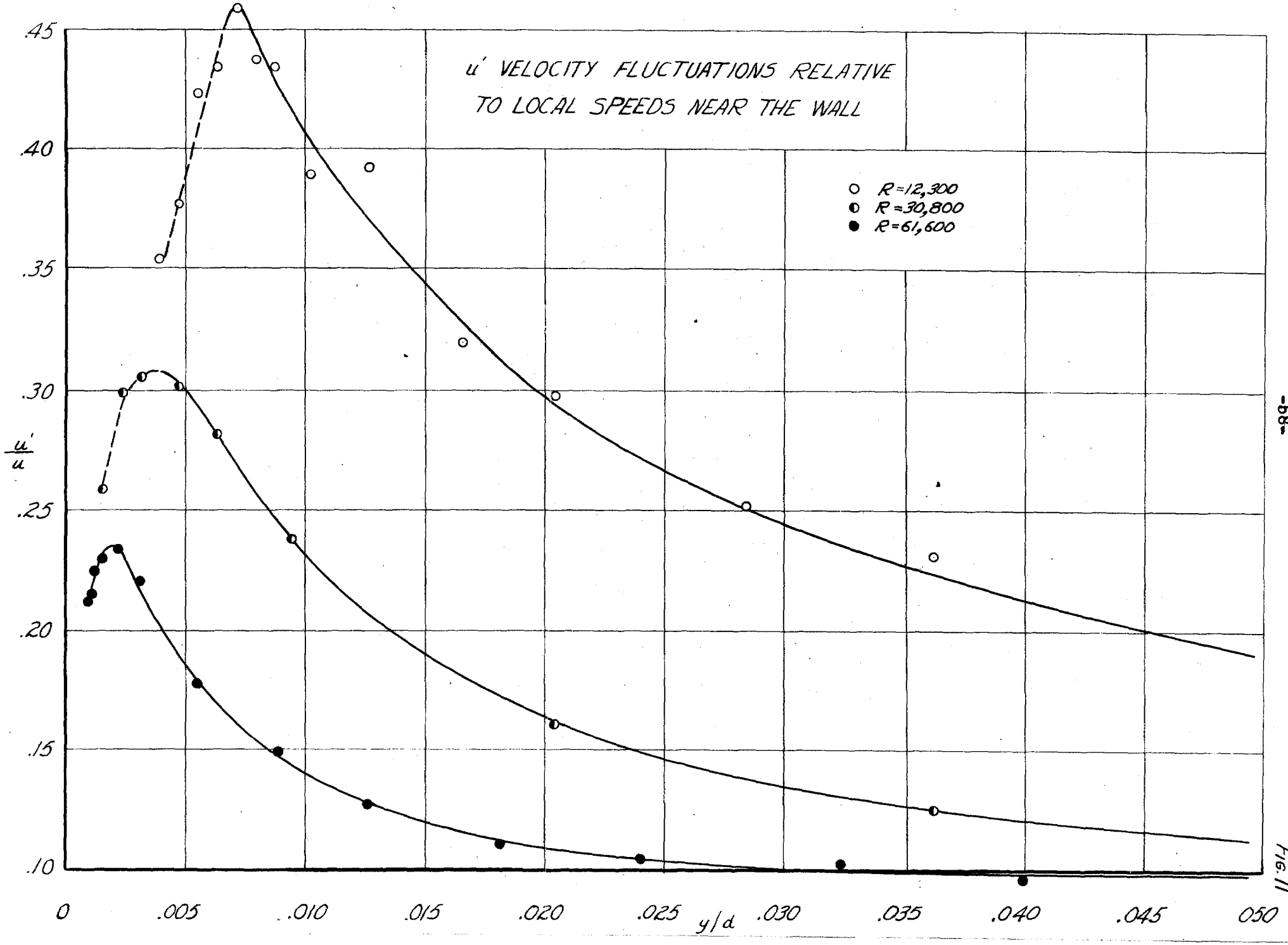
u' VELOCITY FLUCTUATIONS RELATIVE TO LOCAL SPEEDS NEAR THE WALL
R=12,300
R=30,800
R=61,600
.45
.40
.35
.30
.25
.20
.15
.10
u'/u
0
.005
.010
.015
.020
.025
y/d
.030
.035
.040
.045
050

FIG. 11

FIG. 12

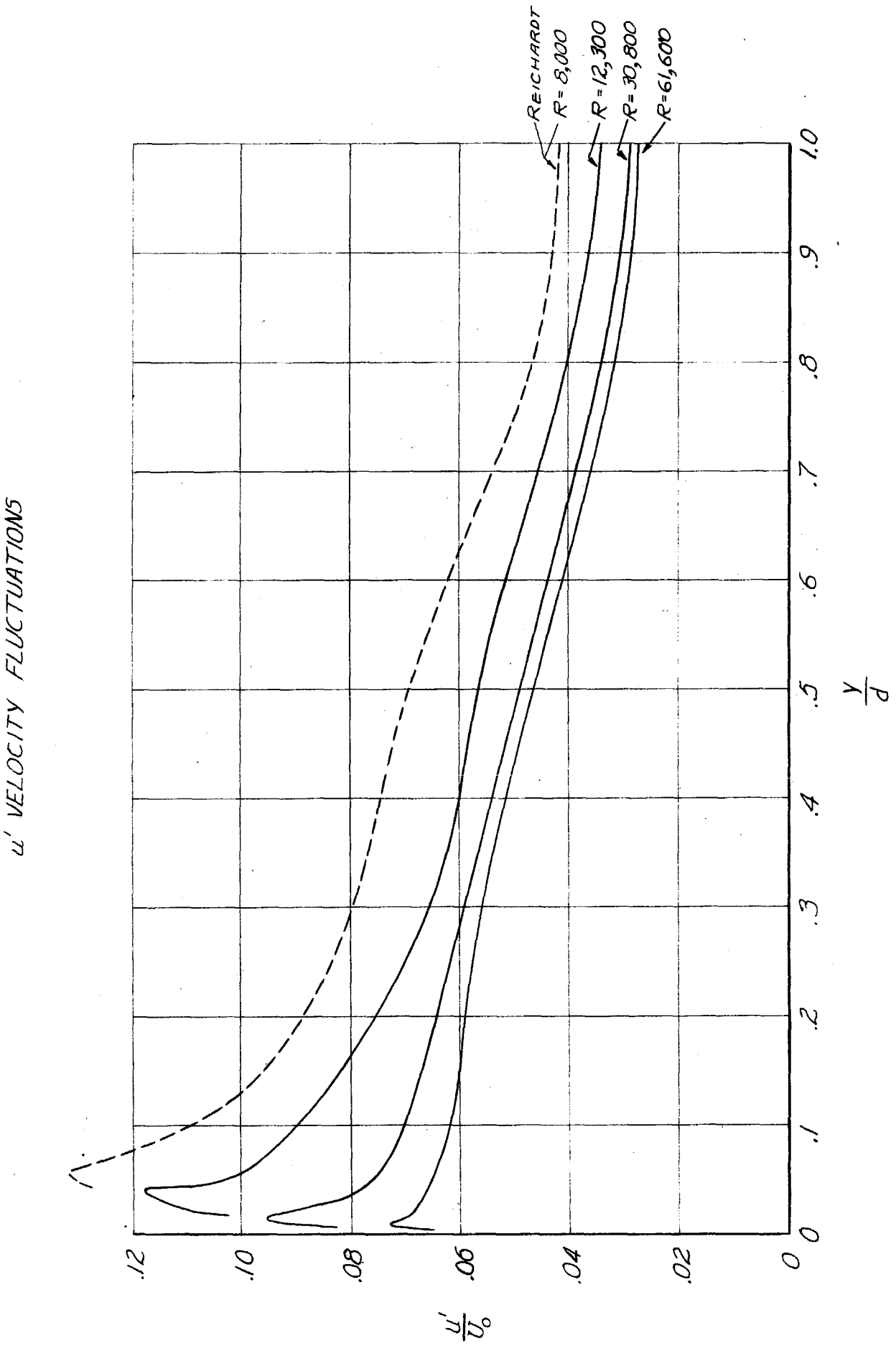
u' VELOCITY FLUCTUATIONS
REICHARDT
R = 8,000
R = 12,300
R = 30,800
R = 61,600
.12
.10
.08
.06
.04
.02
0
u'/U₀
0
.1
.2
.3
.4
.5
.6
.7
.8
.9
1.0
y/d

FIG. 13

u' VELOCITY FLUCTUATIONS NEAR THE WALL

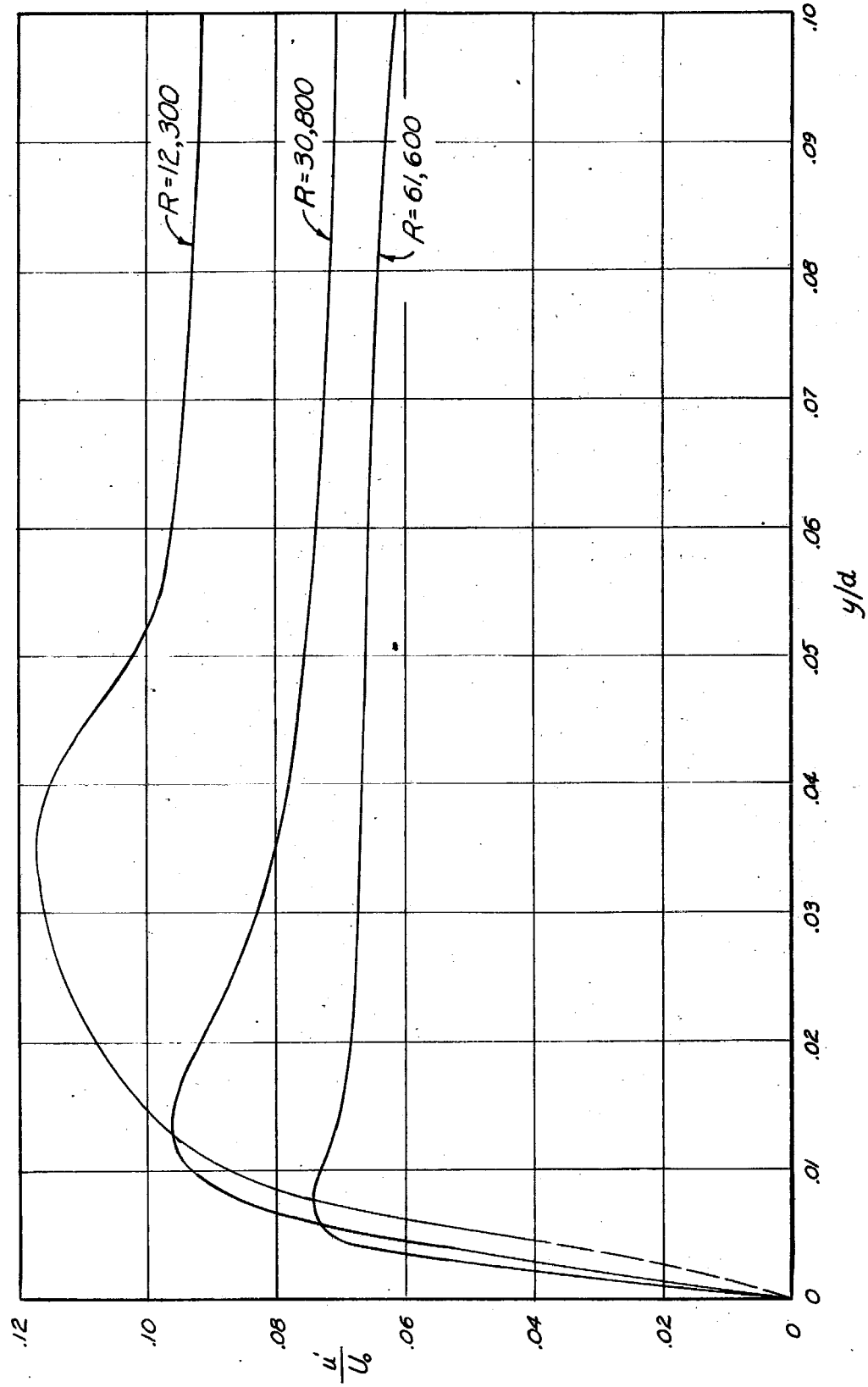

FIG. 14

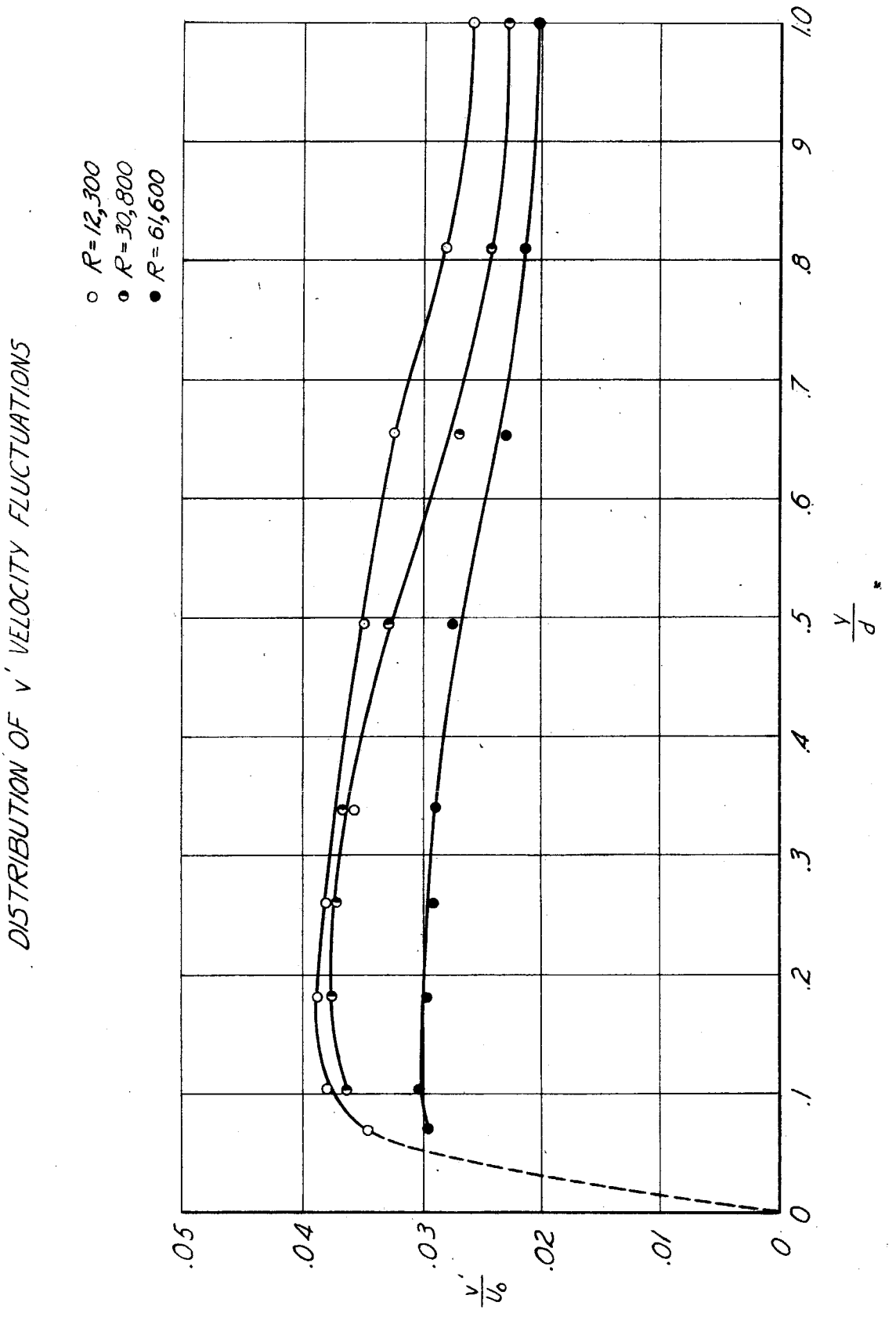
DISTRIBUTION OF v' VELOCITY FLUCTUATIONS
○ R=12,300
◉ R=30,800
● R=61,600
.05
.04
.03
.02
.01
0
v'/U₀
0
.1
.2
.3
.4
.5
.6
.7
.8
.9
1.0
y/d

Fig. 15

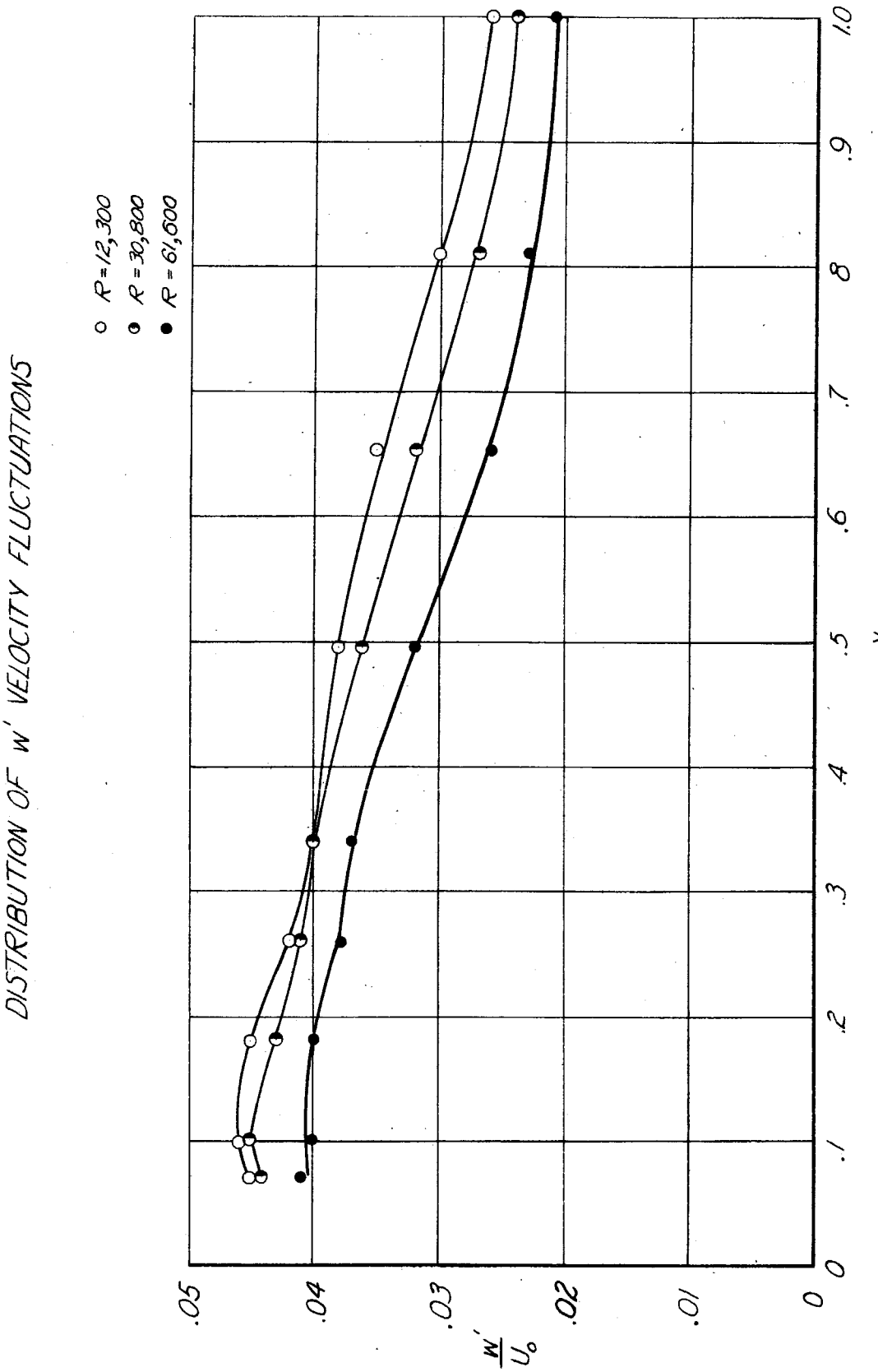
DISTRIBUTION OF w' VELOCITY FLUCTUATIONS
R=12,300
R=30,800
R=61,600
.05
.04
.03
.02
.01
0
w'/U₀
0
.1
.2
.3
.4
.5
.6
.7
.8
.9
1.0
y/d

FIG. 16

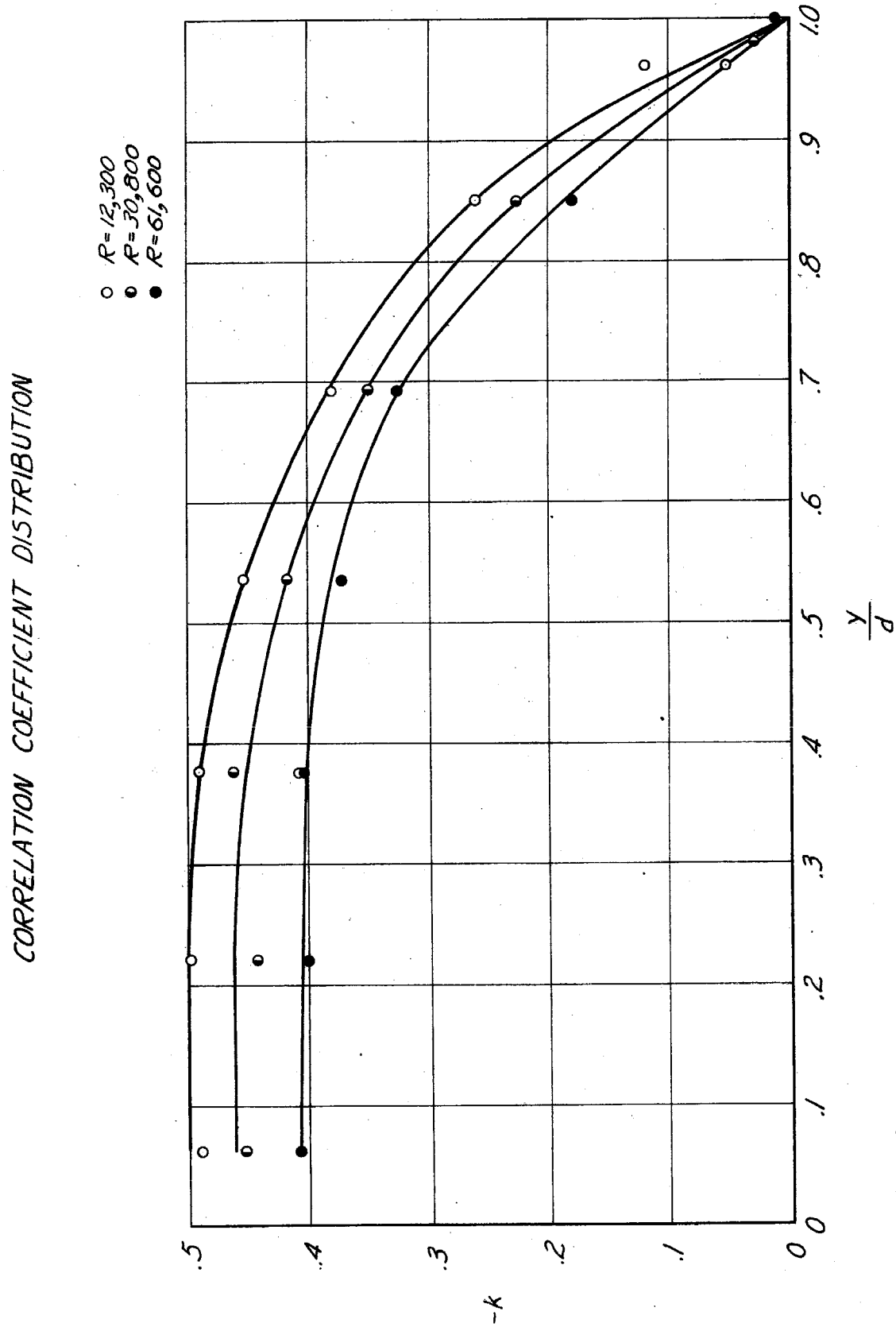
CORRELATION COEFFICIENT DISTRIBUTION
R=12,300
R=30,800
R=61,600
-k
.5
.4
.3
.2
.1
0
y/d
0
.1
.2
.3
.4
.5
.6
.7
.8
.9
1.0

FIG. 17

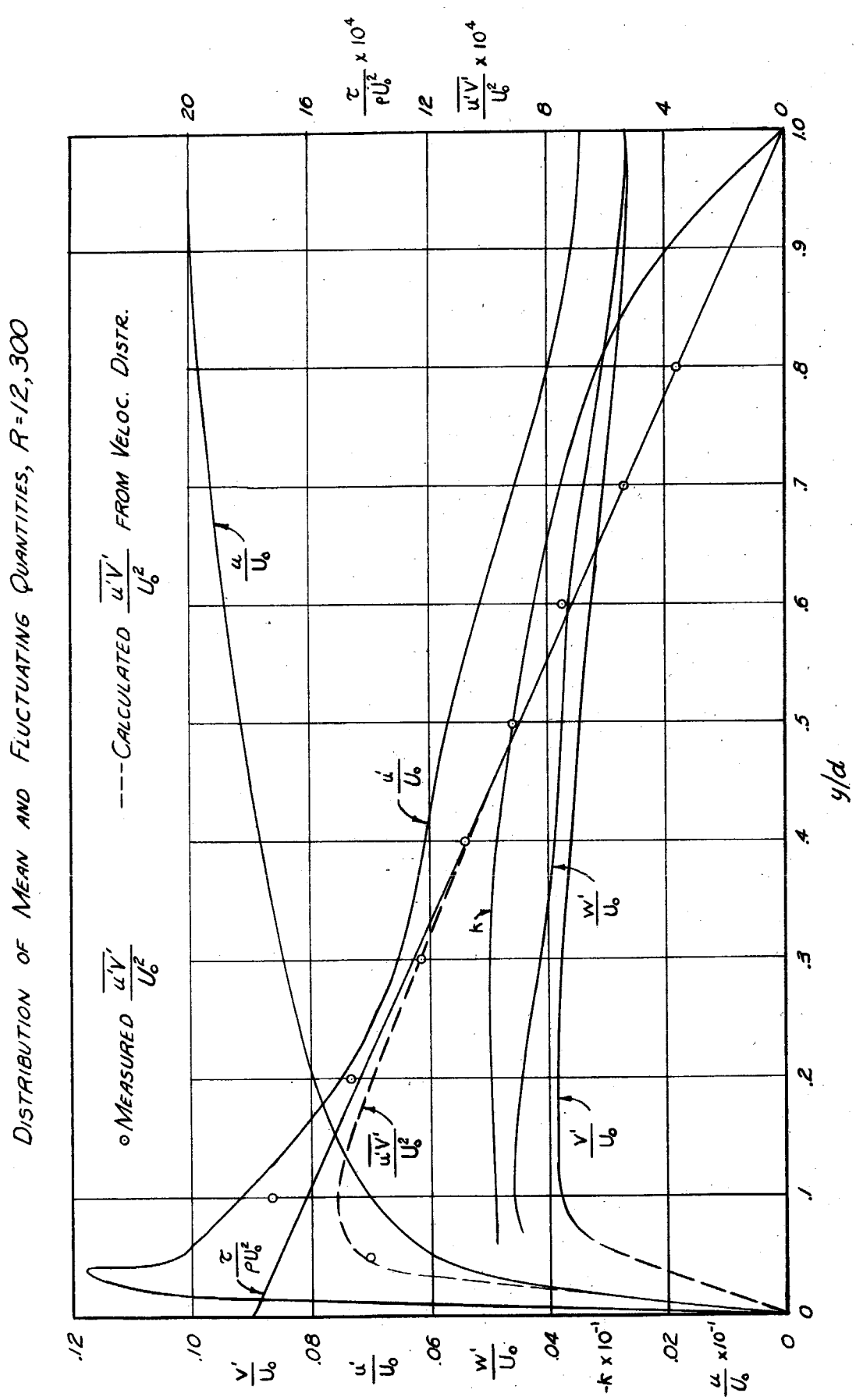
DISTRIBUTION OF MEAN AND FLUCTUATING QUANTITIES, R=12,300
o MEASURED $\frac{\overline{u'v'}}{U_o^2}$
---CALCULATED $\frac{\overline{u'v'}}{U_o^2}$ FROM VELOC. DISTR.
$\frac{u}{U_o}$
$\frac{u'}{U_o}$
$\frac{\overline{u'v'}}{U_o^2}$
$\frac{\tau}{\rho U_o^2}$
$\frac{v'}{U_o}$
$\frac{w'}{U_o}$
k
y/d
$\frac{\tau}{\rho U_o^2} \times 10^4$
$\frac{\overline{u'v'}}{U_o^2} \times 10^4$
$-k \times 10^{-1}$
$\frac{u}{U_o} \times 10^{-1}$

Fig. 18

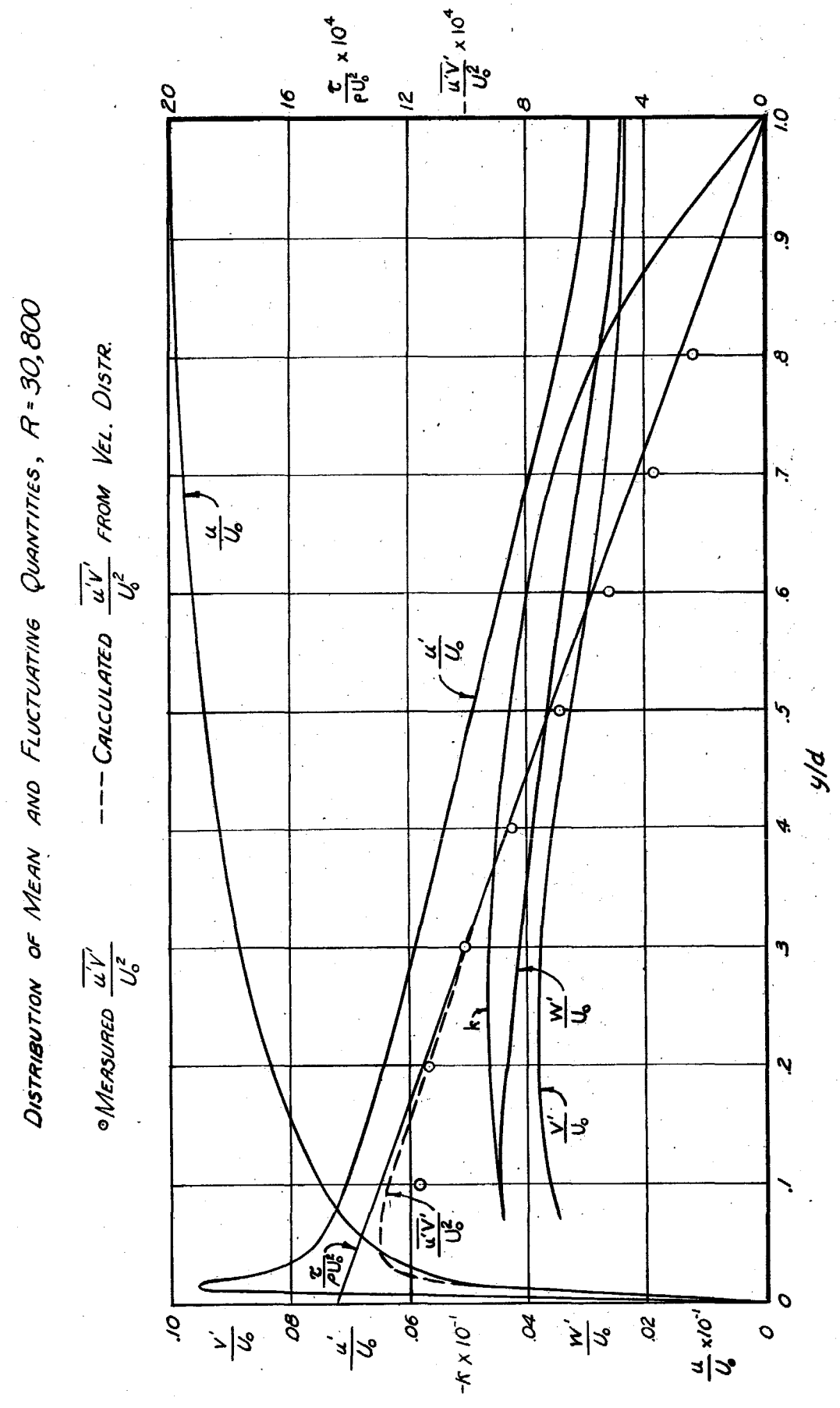
DISTRIBUTION OF MEAN AND FLUCTUATING QUANTITIES, R = 30,800
○ MEASURED $\frac{\overline{u'v'}}{U_o^2}$
--- CALCULATED $\frac{\overline{u'v'}}{U_o^2}$ FROM VEL. DISTR.
$\frac{u}{U_o}$
$\frac{u'}{U_o}$
$\frac{v'}{U_o}$
$\frac{w'}{U_o}$
$\frac{\tau}{\rho U_o^2}$
$-\frac{\overline{u'v'}}{U_o^2}$
$\frac{\tau}{\rho U_o^2} \times 10^4$
$-\frac{\overline{u'v'}}{U_o^2} \times 10^4$
$-K \times 10^{-1}$
y/d

FIG. 19

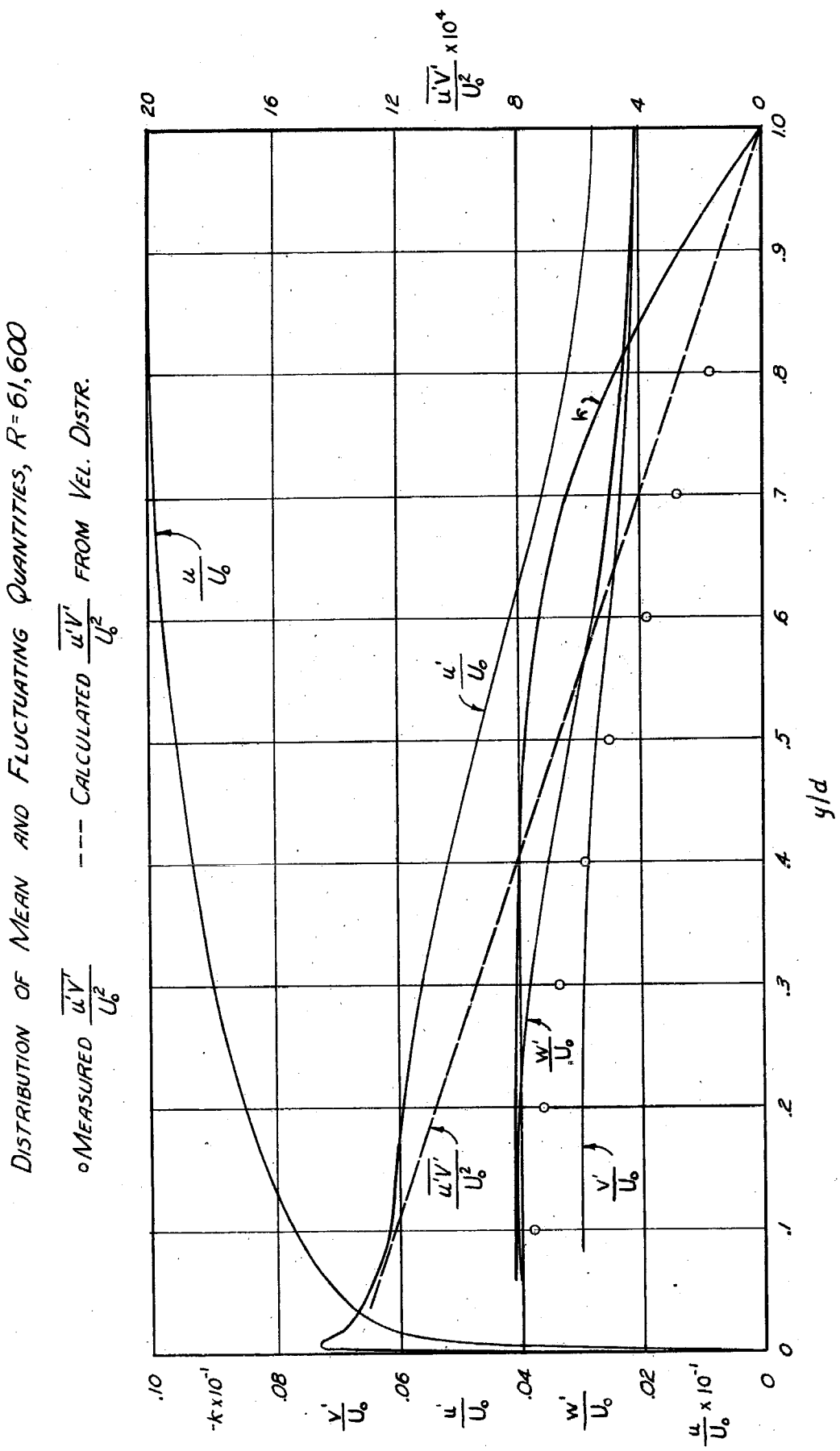
DISTRIBUTION OF MEAN AND FLUCTUATING QUANTITIES, R = 61,600
o MEASURED $\frac{\overline{u'v'}}{U_o^2}$
--- CALCULATED $\frac{\overline{u'v'}}{U_o^2}$ FROM VEL. DISTR.
$\frac{u}{U_o}$
$\frac{u'}{U_o}$
$\frac{\overline{u'v'}}{U_o^2}$
$\frac{w'}{U_o}$
$\frac{v'}{U_o}$
k
$\frac{\overline{u'v'}}{U_o^2} \times 10^4$
$-k \times 10^{-1}$
$\frac{v'}{U_o}$
$\frac{u}{U_o}$
$\frac{w'}{U_o}$
$\frac{u}{U_o} \times 10^{-1}$
y/d

FIG. 20

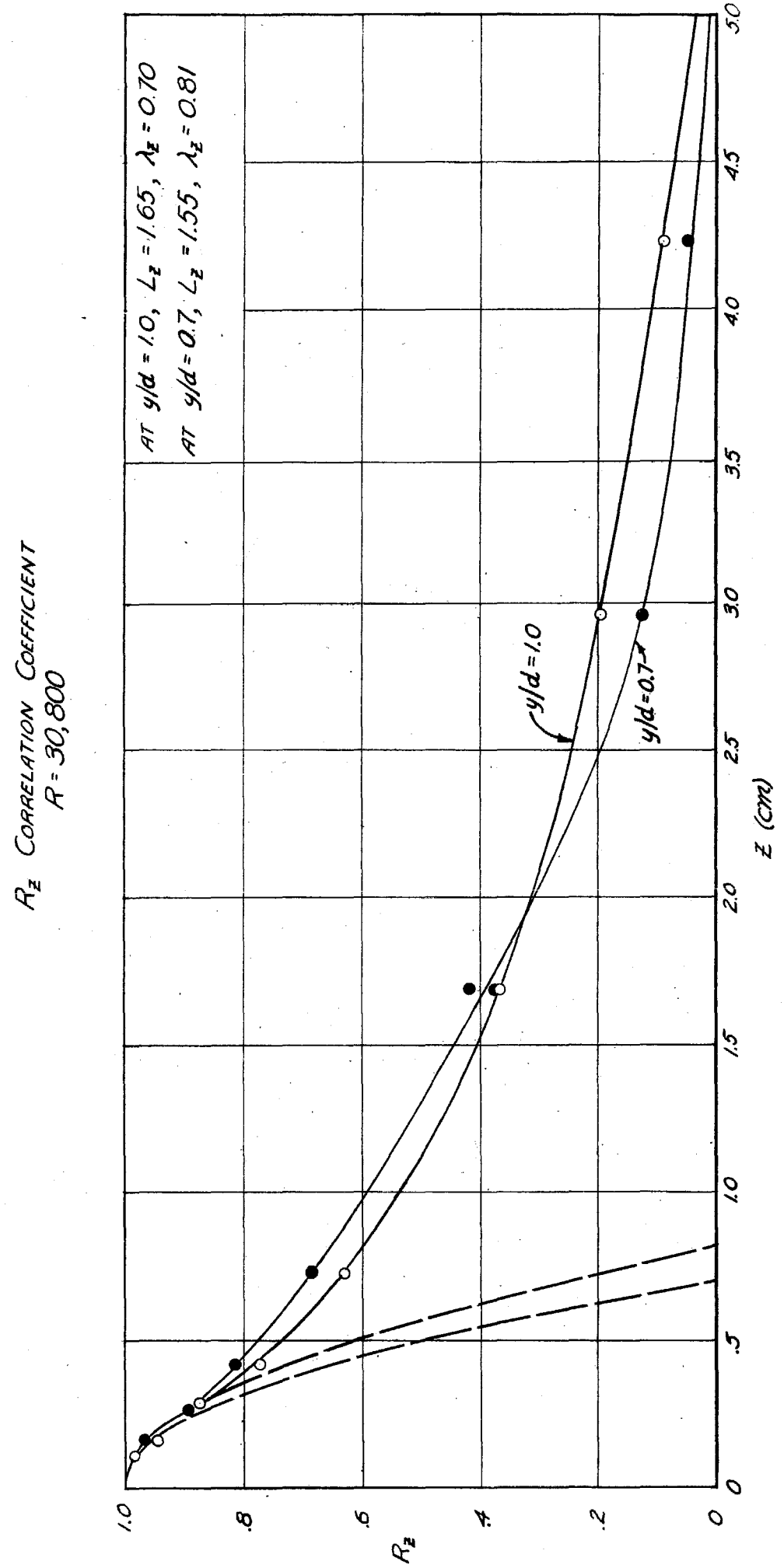
R_z CORRELATION COEFFICIENT
R = 30,800
AT y/d = 1.0, L_z = 1.65, λ_z = 0.70
AT y/d = 0.7, L_z = 1.55, λ_z = 0.81
y/d = 1.0
y/d = 0.7
R_z
1.0
.8
.6
.4
.2
0
z (cm)
0
.5
1.0
1.5
2.0
2.5
3.0
3.5
4.0
4.5
5.0

FIG. 21

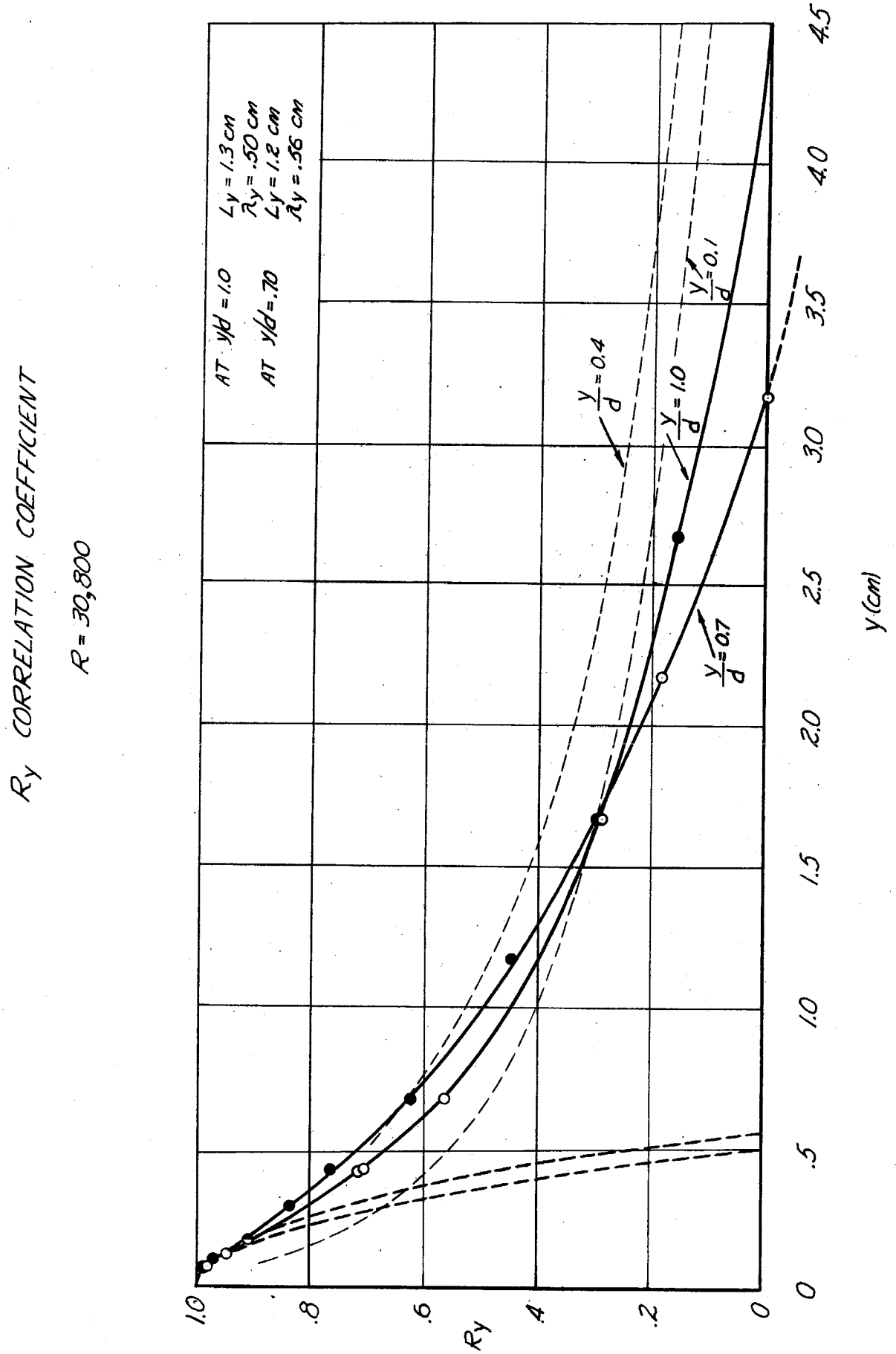
R_y CORRELATION COEFFICIENT
R = 30,800
AT y/d = 1.0 L_y = 1.3 cm
λ_y = .50 cm
AT y/d = .70 L_y = 1.2 cm
λ_y = .56 cm
$\frac{y}{d}$ = 0.4
$\frac{y}{d}$ = 1.0
$\frac{y}{d}$ = 0.1
$\frac{y}{d}$ = 0.7
R_y
y (cm)
1.0
.8
.6
.4
.2
0
0
.5
1.0
1.5
2.0
2.5
3.0
3.5
4.0
4.5

FIG. 22

SCALE OF TURBULENCE DISTRIBUTION

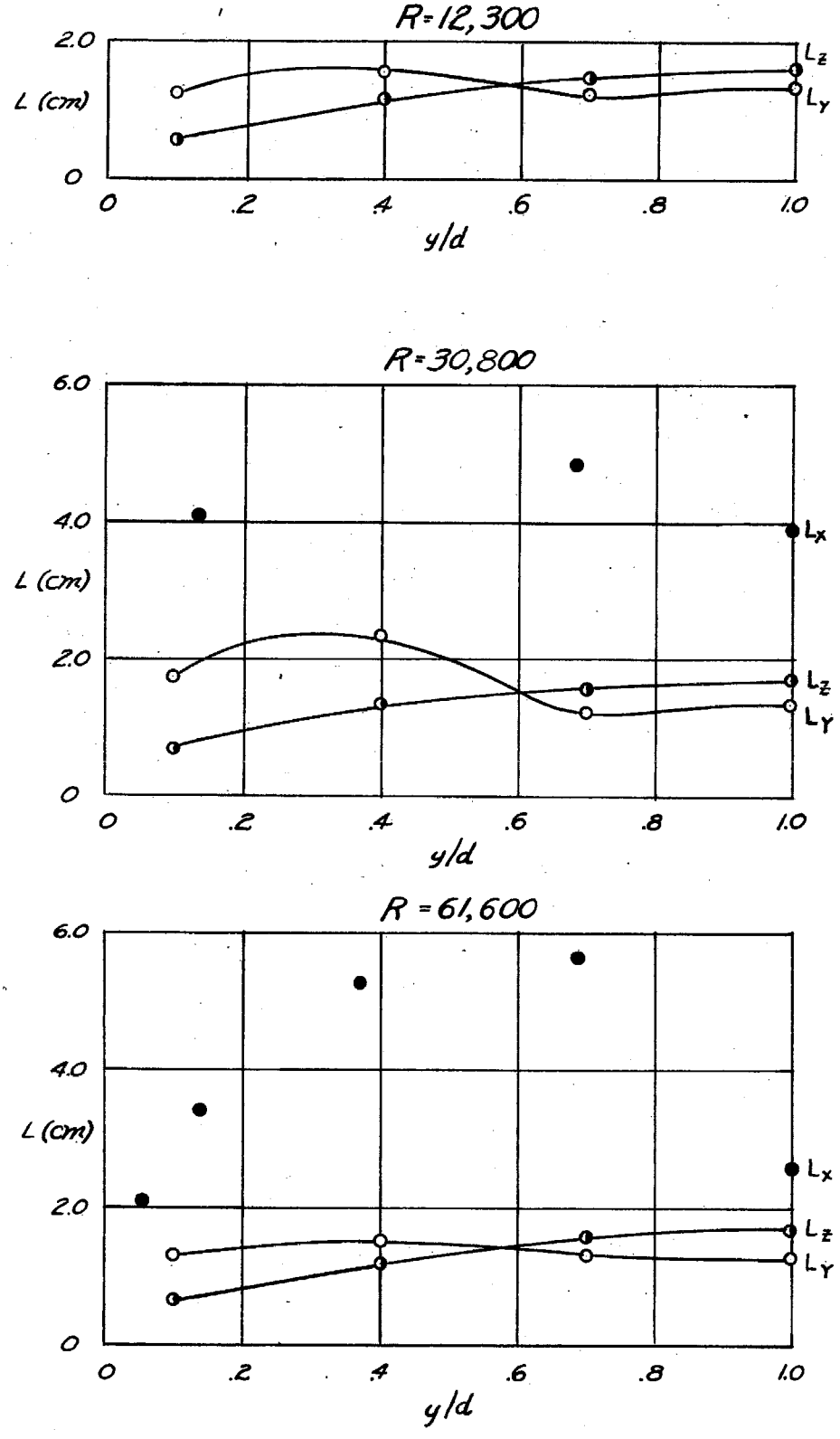

Fig. 23

Microscale of Turbulence Distribution

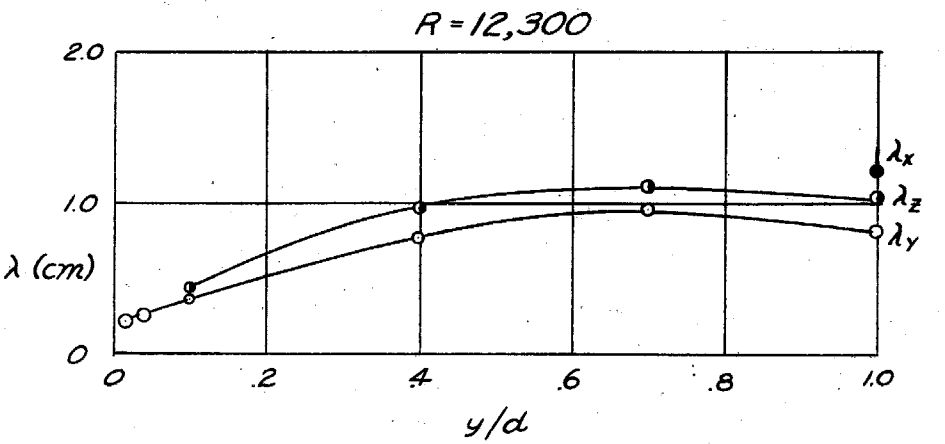

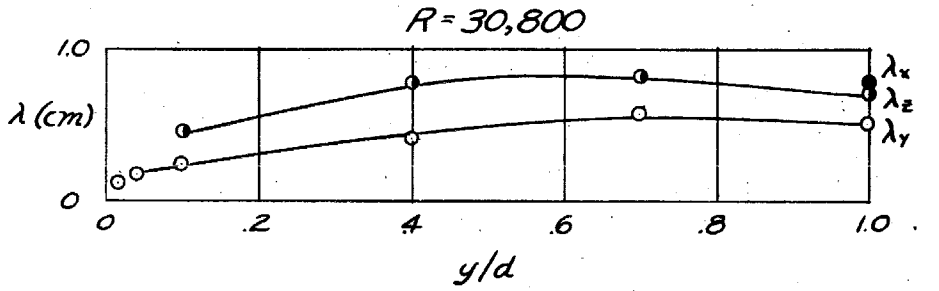

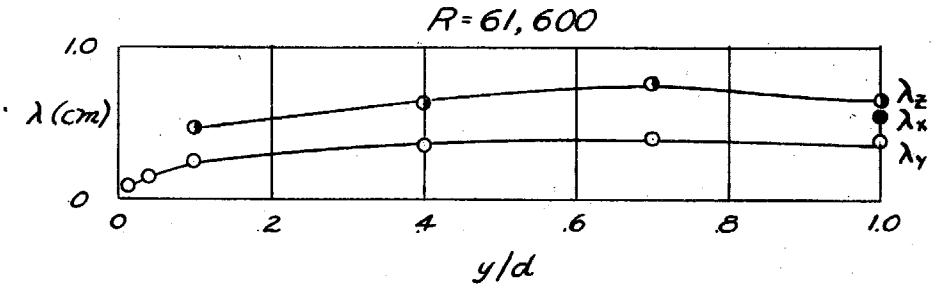

FIG. 24

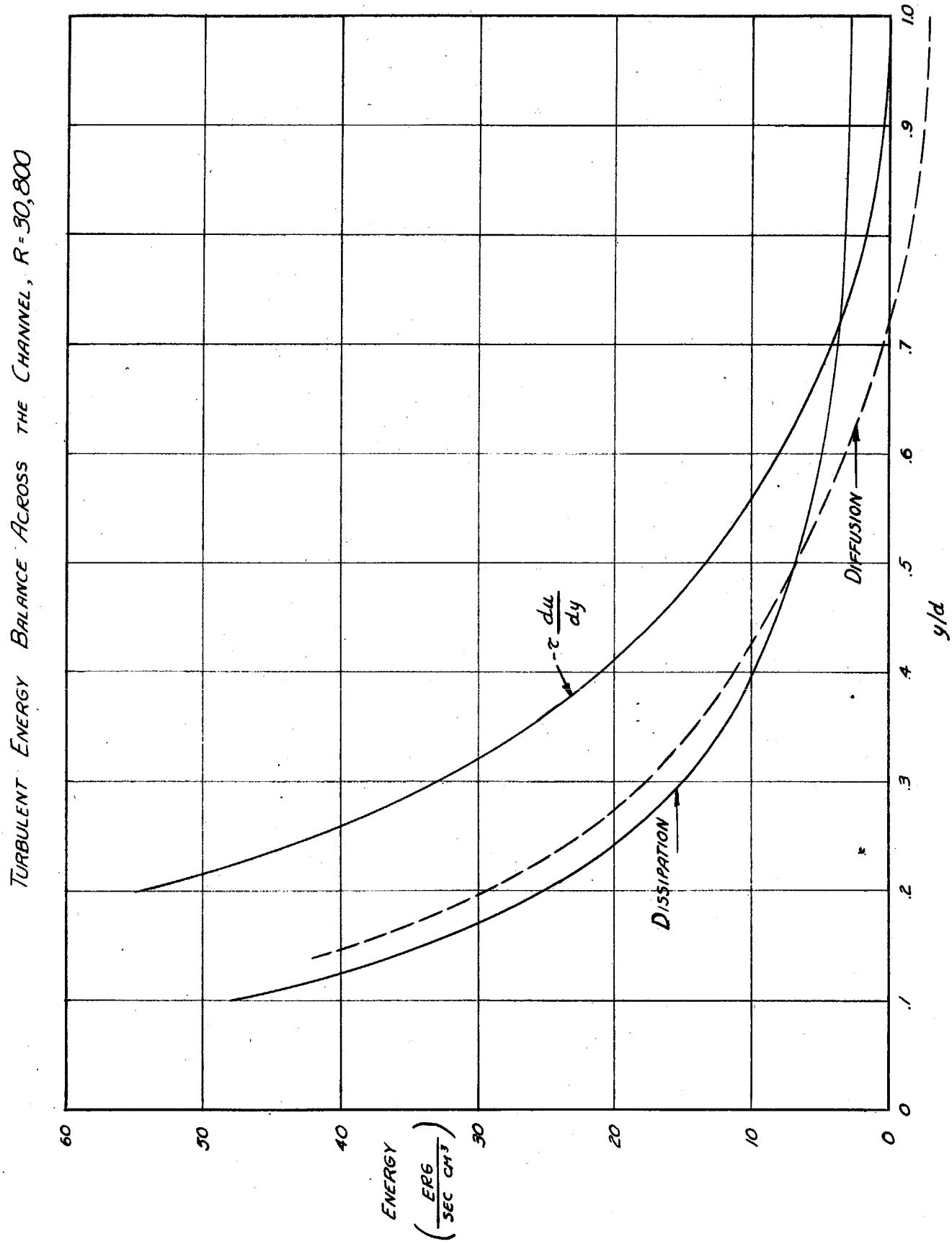
TURBULENT ENERGY BALANCE ACROSS THE CHANNEL, R = 30,800
ENERGY (ERG / SEC CM³)
60
50
40
30
20
10
0
0
.1
.2
.3
.4
.5
.6
.7
.9
1.0
y/d
$-\tau \frac{du}{dy}$
DISSIPATION
DIFFUSION

FIG. 25

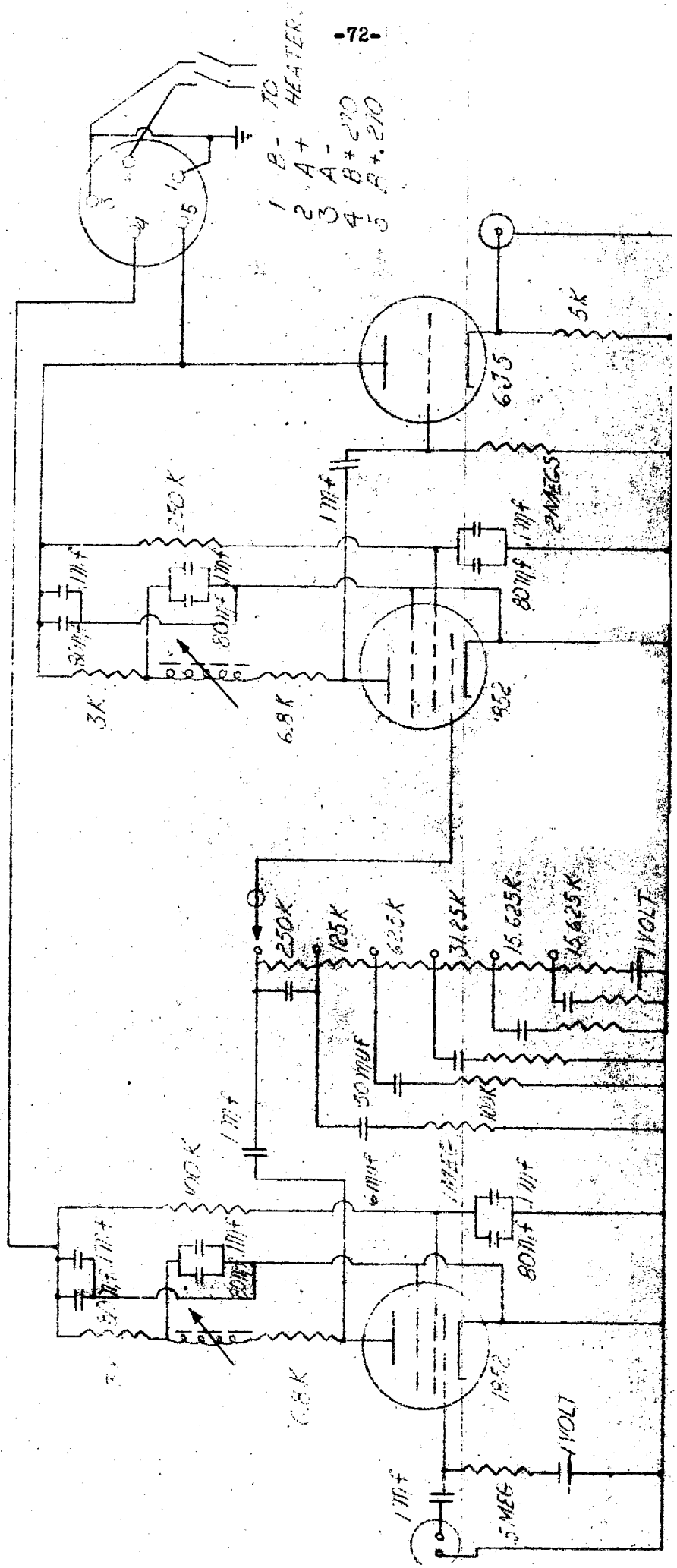

HOT WIRE IRRE-AMPLIFIER

FIG. 26

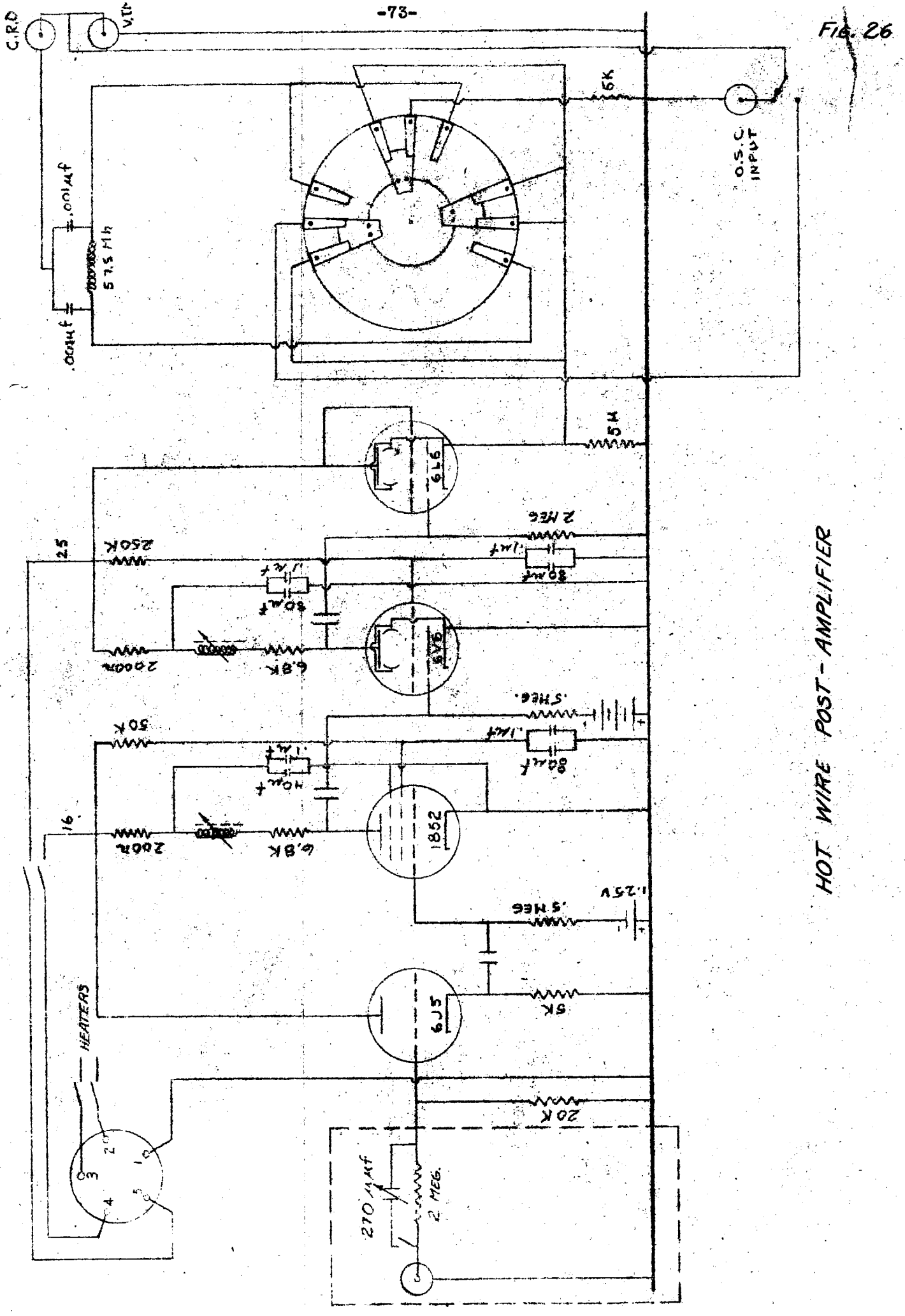

HOT WIRE POST-AMPLIFIER